J Neurophysiol
88: 1634–1654, 2002; 10.1152/jn.00064.2002.

Long-Range Synchronization of γ and β Oscillations and the Plasticity of Excitatory and Inhibitory Synapses: A Network Model

ANDREA BIBBIG,[1] ROGER D. TRAUB,[1] AND MILES A. WHITTINGTON[2]
[1]*Department of Physiology and Pharmacology, State University of New York Health Science Center, Brooklyn, New York 11203; and* [2]*School of Biomedical Sciences, University of Leeds, Leeds LS2 9NL, United Kingdom*

Received 31 January 2002; accepted in final form 10 June 2002

Bibbig, Andrea, Roger D. Traub, and Miles A. Whittington. Long-range synchronization of γ and β oscillations and the plasticity of excitatory and inhibitory synapses: a network model. *J Neurophysiol* 88: 1634–1654, 2002; 10.1152/jn.00064.2002. The ability of oscillating networks to synchronize despite significant separation in space, and thus time, is of biological significance, given that human γ activity can synchronize over distances of several millimeters to centimeters during perceptual and learning tasks. We use computer simulations of networks consisting of excitatory pyramidal cells (e-cells) and inhibitory interneurons (i-cells), modeling two tonically driven assemblies separated by large ($\geq$8 ms) conduction delays. The results are as follows. *1*) Two assemblies separated by large conduction delays can fire synchronously at β frequency (with i-cells firing at γ frequency) under two timing conditions: e-cells of (say) assembly 2 are still inhibited "delay + spike generation milliseconds" after the e-cell beat of assembly 1; this means that the e-cell inhibitory postsynaptic potential (IPSP) cannot be significantly shorter than the delay (2-site effect). This implies for a given decay time constant that the interneuron $\rightarrow$ pyramidal cell conductances must be large enough. The e-cell IPSP must last longer than the i-cell IPSP, i.e., the interneuron $\rightarrow$ pyramidal cell conductance must be sufficiently large and the interneuron $\rightarrow$ interneuron conductance sufficiently small (local effect). *2*) We define a "*long-interval doublet*" as a pair of interneuron action potentials—separated by approximately "delay milliseconds"—in which *a*) the first spike is induced by tonic inputs and/or excitation from nearby e-cells, while *b*) the second spike is induced by (delayed) excitation from distant e-cells. "*Long-interval population doublets*" (long-interval doublets of the i-cell population) are necessary for synchronized firing in our networks. Failure to produce them leads to almost anti-phase activity at γ frequency. *3*) An (almost) anti-phase oscillation is the most stable oscillation pattern of two assemblies that are separated by axonal conduction delays of approximately one-half a γ period (delays from 8 to 17 ms in our simulations) and that are firing at γ frequency. *4*) Two assemblies separated by large conduction delays can synchronize their activity with the help of interneuron plasticity. They can also synchronize without pyramidal cell $\rightarrow$ pyramidal cell connections being present. The presence of pyramidal cell $\rightarrow$ pyramidal cell connections allows, however, for synchronization if other parameters are at inappropriate values for synchronization to occur. *5*) Synchronization of two assemblies separated by large conduction delays with the help of interneuron plasticity is not simply due to slowing down of the oscillation frequency. It is reached with the help of a "*synchronizing-weak-beat*," which induces sudden changes in the oscillation period length of the two assemblies.

INTRODUCTION

Sensory processing involves several brain areas, and within each area, several groups of neurons. It has been proposed that the neuronal assemblies representing different parts of one "object" are bound together by synchronous oscillatory activity in the γ (30–70 Hz) and/or β (10–29 Hz) range (e.g., Gray 1994; Singer and Gray 1995; Tallon-Baudry et al. 1999). Stimulus-specific synchronized γ activity has, for example, been reported in the visual cortex of the anesthetized cat (Eckhorn et al. 1988; Gray and Singer 1989; Gray et al. 1989) and in the awake monkey (Eckhorn et al. 1993; Frien et al. 1994; Kreiter and Singer 1996). Stimulus-specific synchronized γ or γ/β activity has also been shown in the human brain during perceptual and learning tasks (Tallon-Baudry et al. 1998, 1999, 2001; von Stein et al. 1999), and most interestingly, synchronization was reported despite separation between participating areas of several millimeters and up to several centimeters (Desmedt and Tomberg 1994; Miltner et al. 1999; Tallon-Baudry 2001). Areas separated by distances of several centimeters are likely to be connected by fast cortico-cortical connections, although the relevant axonal conduction delays are not known. However, axonal collaterals within the gray matter are reported to conduct with axonal conduction velocities as small as 0.1 mm/ms (Aroniadou and Keller 1993). Thus even spatial separations of 3–4 mm (common for extrinsic collaterals; Rockland and Drash 1996), or of 3–6 mm (common for intrinsic, i.e., within-area, collaterals; K. Rockland, personal communication) lead to large temporal separations, in principle up to 60 ms. Because synchronization has been reported over these distances, there must be a mechanism for synchronizing neocortical neuronal assemblies despite significant separation in space and/or very large conduction delays.

Kopell et al. (2000) showed that, while two assemblies separated by 10 ms or more could synchronize during a β oscillation, they could not stably synchronize during a γ oscillation [by "β oscillation" we mean an oscillation with inhibitory cells (i-cells) firing at γ frequency while excitatory cells (e-cells) skip beats and thus only fire at β frequency]. This was

Address for reprint requests: A. Bibbig, SUNY Health Science Center, Dept. of Physiology and Pharmacology, 450 Clarkson Ave., Box 31, Brooklyn, NY 11203 (E-mail: andrea.bibbig@downstate.edu).

The costs of publication of this article were defrayed in part by the payment of page charges. The article must therefore be hereby marked "*advertisement*" in accordance with 18 U.S.C. Section 1734 solely to indicate this fact.

shown mathematically and using simulations with conductance-based models, not including, however, synaptic plasticity. Other studies have reported that synchronization was unreliable if axonal conduction delays of more than 6 ms were involved (Ritz et al. 1994), or that synchronization could be achieved despite larger conduction delays if the carrier frequency was slow enough (König and Schillen 1991). Again, the synapses used in these studies were not plastic.

Preliminary modeling studies using networks of simple (Bibbig 1998, 1999, 2000; Bibbig and Traub 2000) and detailed compartmental neuronal models (Bibbig et al. 2001) showed that synchronization with axonal conduction delays of 10 ms and more can be achieved with the help of interneuron plasticity (the plasticity of reciprocal pyramidal/interneuron conductances, usually in this paper referred to as e → i and i → e synapses). In Bibbig et al. (2001), potentiation of i → e synapses is replaced by growing afterhyperpolarizations (AHPs) in pyramidal cells but not in interneurons. This is possible even though average axonal conduction delays ≥8 ms force the two assemblies to fire with large phase lags, leading to an almost anti-phase activity, shortly after the beginning of the oscillation. But with a so-called *"synchronizing-weak-beat"* (γ beat with sparse i- and e-cell activity), the oscillation can switch from almost anti-phase to near-synchrony. In Bibbig (1999, 2000), Bibbig and Traub (2000), and Bibbig et al. (2001), we introduced the phenomenon of a synchronizing-weak-beat and named it "i-weak beat," referring to its sparse i-cell activity. However, we now call it a "synchronizing-weak-beat" to emphasize its function, and because not only i-cell, but also e-cell, activity is sparse during such a beat. We will explain in RESULTS and Fig. 11 exactly how a synchronizing-weak-beat can lead to synchronization.

In this paper, we extend the analysis of Bibbig et al. (2001) by examining more closely the mechanism with which interneuron plasticity leads to changes in synaptic conductances that can generate a *synchronizing-weak-beat* and how this *synchronizing-weak-beat* in turn can synchronize two assemblies that have been firing almost in anti-phase. For these "long-range synchronization after almost anti-phase activity" simulations, we use a different kind of network model than in Bibbig et al. (2001), namely a network of simple integrate-and-fire neurons with refractory mechanism. This is to show that the ability to synchronize is not dependent on "fancy" mechanisms but depends on simple mechanisms inherent in networks of virtually all types of neuronal models. And we show that purely local i → e conductances are sufficient to generate synchrony, meaning that not even a few between-assembly i → e conductances (as used in the detailed network model here and in Bibbig et al. 2001) are necessary. In addition to these simulations with the simple network model, we present new data showing that the synchronized oscillations generated here with long conduction delays share some characteristics with tetanically induced β oscillations: they are at β frequency and they show missed e-cell beats (see Traub et al. 1999). However, they also have a feature in common with synchronous γ oscillations with short conduction delays: they are not dependent on e → e synapses (see also Kopell et al. 2000; Traub et al., 1999), although the synchronization process is accelerated if e → e synapses are present. (Thus in vivo, e → e synapses are probably involved in this synchronization process.) We show that long-range synchronization at β frequency depends, however, on e-cells of one assembly projecting to the other assembly's i-cells (i.e., e → i connections). We point out conditions under which *synchronizing-weak-beat*s and synchronization can take place. In addition, we will examine which time-independent parameters influence the synchrony behavior, i.e., lead to immediate synchrony or to almost anti-phase behavior. Some important parameters in this regard are as follows: amplitude/duration of pyramidal cell inhibitory postsynaptic potential (IPSP) in relation to interneuron IPSP, or in more technical terms, i → e conductance relative to i → i conductance and relative to the delay, or alternatively, the e-cell AHP in relation to the i-cell AHP. Furthermore, we introduce the concept of a *"long-interval doublet"* (a pair of interneuron action potentials—separated by approximate "delay milliseconds"—in which the first spike is induced by tonic inputs and/or excitation from nearby e-cells, whereas the second spike is induced by (delayed) excitation from distant e-cells). And we show that *"long-interval population doublets"* (long-interval doublets of the i-cell population) are necessary for synchronized firing of two assemblies separated by long axonal conduction delays in our networks. Failure to produce them leads to almost anti-phase activity at γ frequency. Finally, we will analyze why two assemblies, separated by a conduction delay of approximately one-half a γ period (depending on the exact network model: γ period 20–25 ms, average delay 8–17 ms), if they are firing at γ frequency, will "like to fire" and thus be stabilized in an almost anti-phase γ oscillation. Such an oscillation persists if no *synchronizing-weak-beats* can occur.

Some of these data have been published in abstract form (Bibbig 1998, 1999; Bibbig and Traub 2000).

METHODS

We used two network models in the simulations shown in this paper: a "detailed" model consisting of a large network of detailed (multicompartment) neurons (Fig. 1) and a "simple" model with a (relatively) small network of simple integrate-and-fire neurons (Fig. 2).

Detailed network model

The detailed network model is almost identical to the model used and described in detail in Bibbig et al. (2001). Thus here we will concentrate on summarizing the most important principles of this network model and emphasizing the few differences between the two models.

The most important characteristic of our network is that we use self-organized Hebbian plasticity for modifying synaptic conductances. This means that, as in Bibbig et al. (2001), synapses from excitatory pyramidal cells to other pyramidal cells and to inhibitory interneurons (i.e., e → e and e → i synapses) are modifiable, in Hebbian fashion, on the time scale of the oscillations, i.e., tens to hundreds of milliseconds. In addition, in some simulations (e.g., Fig. 8) i → e synapses are modifiable according to a Hebbian learning rule. The plasticity of excitatory and inhibitory synapses was motivated by earlier simulations (Bibbig 1998, 1999, 2000) in networks of integrate-and-fire neurons, as well as by recent experimental data of plasticity of excitatory and inhibitory synapses in hippocampal slices during tetanus-induced γ and β oscillations (e.g., Whittington et al. 1997b for e → e; Bibbig et al., 2001 for e → i; M. A. Whittington, unpublished data, for potentiation of i → e conductance; note, however, that changes in i → e synaptic connections are difficult to isolate and document experimentally during network γ or β oscillations: this is the case because isolation of IPSPs requires blockade of AMPA

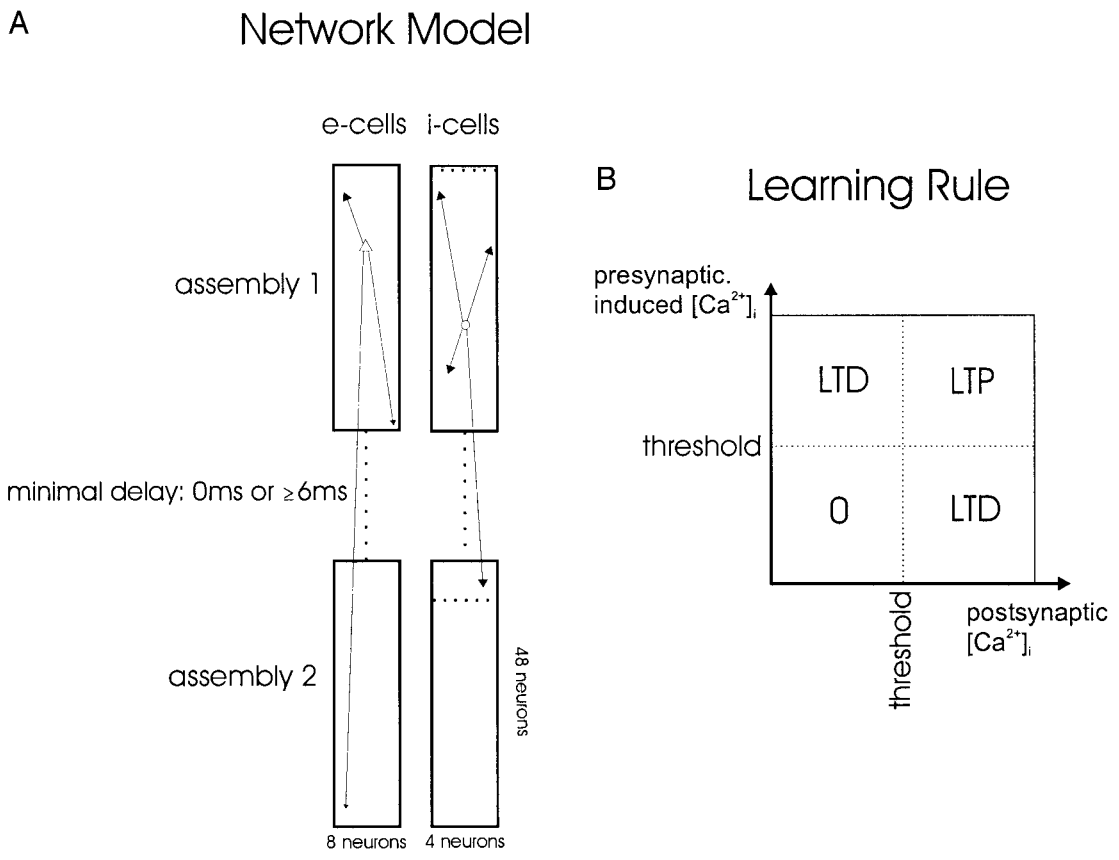

FIG. 1. *A*: detailed network model consists of 768 excitatory and 384 inhibitory compartmental neurons, arranged in 2 blocks, constituting assemblies 1 and 2, respectively. The 2 assemblies are separated by a minimum delay: 0 ms in simulations modeling nearby assemblies in hippocampal slices (as in Fig. 3*A*), ≥6 ms in simulations modeling long-range synchronization (10 and 15 ms in the simulations shown in this paper). Excitatory pyramidal cells ("e-cells") project globally with a probability exponentially decreasing depending on distance (illustrated by the distance-dependent arrow size), whereas inhibitory interneurons ("i-cells") project only locally to approximately one-half the array. *B*: learning rule for e → e and e → i (in some simulations, i → e) synapses is Hebbian depending on presynaptically induced and postsynaptic $[Ca^{2+}]_i$.

receptors; but block of AMPA receptors prevents γ and β portions of the oscillation from occurring in a normal way; Traub et al. 1999). There are also data that document interneuron plasticity in hippocampus and in neocortex, generated by different stimulation paradigms (e.g. Ouardouz and Lacaille 1995; Perez et al. 2001; Rozov et al. 1998 for plasticity of e → i synapses; Holmgren and Zilberter 2001; Perez et al. 1999 as examples of i → e plasticity in hippocampus and in neocortex, respectively).

There are three differences with the large, detailed model used in Bibbig et al. 2001.

1. The neuronal network was split into two "blocks," separated by ≥10-ms conduction delay throughout all simulations shown in this paper, to examine long-range synchronization. A *minimum* delay of 10 ms is equivalent to an *average* delay of 12 ms between the two assemblies. This average delay is the value usually provided in RESULTS and Fig. 1. In addition to the simulations shown in this paper (12- and 17-ms average delay), we performed numerous additional simulations with many other delays. The network behavior described in this paper, i.e., almost anti-phase activity at γ frequency and synchronous activity at β frequency showing missed e-cell beats, is produced for average conduction delays ≥ 8 ms, i.e., a minimum delay ≥6 ms (Fig. 1*A*).
2. A fixed i → e conductance was varied from simulation to simulation, or else i → e plasticity was incorporated (as already mentioned above), to investigate the role of i → e conductances in long-range synchronization.
3. $g_{K(M)}$ and $g_{K(AHP)}$ were not altered during the oscillation, to isolate i → e conductance effects.

All other parameters are as described in detail in Bibbig et al. 2001. The most important features of the model (including the above mentioned 3 differences) are summarized in the following paragraphs.

Condensed description of the most important features of the model

OVERALL NETWORK STRUCTURE. The network contains 768 excitatory pyramidal cells ("e-cells") and 384 inhibitory interneurons ("i-cells"). As seen in Fig. 1, the pyramidal cells are arranged into two 48 × 8 blocks representing two stripes of neuronal tissue. The interneurons are arranged into two blocks of 48 × 4 cells, overlapping the e-cell arrays. The two blocks of e- and i-cells represent two local cortical areas (each of them approximately 1 mm wide), which are separated by a long distance (we conducted simulations with "minimum" long axonal conduction delays between the "innermost ends of the blocks" ranging from 6 to 17 ms; most simulations shown here have minimum conduction delays of 10 ms; in Fig. 4, *C* and *D*, the minimum conduction delay was 15 ms).

INDIVIDUAL NEURONAL PROPERTIES. Each e-cell is a multicompartment object (64 soma-dendritic compartments and 5 axonal ones) containing Na^+, Ca^{2+}, and different sorts of K^+ conductances as originally described in Traub et al. (1994), with the exact values and densities (including the addition of an M-type voltage-dependent K^+ conductance) given in Bibbig et al. (2001).

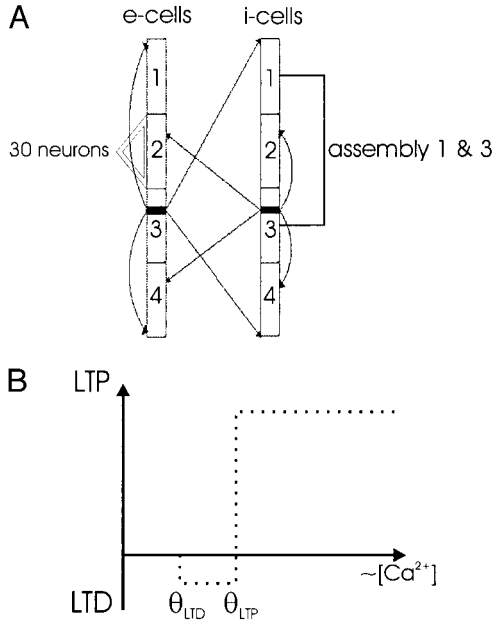

FIG. 2. Block diagram of the simple network model, learning rule, and simulation parameters. *A*: network structure of the simple model consisting of 120 excitatory cells (e-cells) and 120 inhibitory interneurons (i-cells). These cells are each modeled as simple integrate-and-fire neurons with a firing threshold and a refractory period. e-Cells and related i-cells are subdivided into 4 assemblies of 30 cells each. Usually, assemblies 1 and 3 were stimulated together with a tonic input. The goal was to have these assemblies (1 and 3) synchronize to form a "global cell assembly." e-Cell projections are far-reaching, whereas i-cells project only locally, i.e., i-cells of 1 group only form projections to some of the neighboring cells, so that i-cells of group 1 do not project to e- and i-cells of group 3 (this is why usually these 2 assemblies were stimulated together; we wanted to exclude synchronizing long-range i $\rightarrow$ e effects). Spike transmission of all neurons is via distance-dependent axonal conduction delays of 0.5 mm/ms. *B*: learning rule: at all synapses (e $\rightarrow$ e, e $\rightarrow$ i, and i $\rightarrow$ e), we used a Hebbian 2-threshold learning rule (Artola et al. 1990; Bienenstock et al. 1982) with the product of a "presynaptic" [excitatory postsynaptic postential (EPSP) or inhibitory postsynaptic potential (IPSP)] and the postsynaptic signal (spike rate) as a measure. The product should represent the supralinear effect of the EPSP/IPSP and the postsynaptic backpropagating action potential on $[Ca^{2+}]$ of the dendritic spine (Yuste and Denk 1995). If the product exceeded the LTD-threshold, the synaptic weight was decreased by a small amount, Δ. If it was above the LTP-threshold, the weight was increased by 5Δ (e $\rightarrow$ e) or by about 2Δ (e $\rightarrow$ i and i $\rightarrow$ e).

Each i-cell is also a multi-compartment object (46 soma-dendritic compartments and 5 axonal ones), with multiple ionic conductances (as originally described in Traub and Miles 1995), with small differences mentioned in Bibbig et al. (2001).

SYNAPTIC CONNECTIVITY. Each pyramidal cell is contacted by 30 other pyramidal cells and by 80 interneurons (20 "basket cells" from the 1st row, 20 "axo-axonic cells" from the 2nd row, 20 "bistratified cells," and 20 "o/lm cells"). Basket cells contact uniformly the soma and most proximal dendrites of pyramidal cells and dendrites of interneurons. Axo-axonic cells contact the initial segment (most proximal axonal compartment) of pyramidal cells. Bistratified cells and o/lm cells contact the dendrites of pyramidal cells and of interneurons. Each interneuron was excited by 150 pyramidal cells. Interneurons receive 60 inputs from other interneurons, 20 of each sort, with the exception that interneurons are not contacted by axo-axonic cells. For further connectivity details see Bibbig et al. (2001).

Connection probability from presynaptic pyramidal cells to postsynaptic pyramidal cells and interneurons decreased exponentially with a space constant of 1 mm, illustrated by distance-dependent arrow size in Fig. 1*A* (see Csicsvári et al. 1998). The axons of interneurons are constrained to run no further than 500 μm (=25 cell diam) along the long axis of the array; within this domain, interneuron connection probabilities are uniform (again illustrated by uniform arrow size in Fig. 1*A*). This means that here, in the detailed network model, interneurons from assembly 1 may project to i- and e-cells of the neighboring assembly 2 (which is different to the simple model, where interneurons from assembly 1 cannot project to the relevant other assembly 3; see description of the simple network model).

SYNAPTIC ACTIONS. Only AMPA- and $GABA_A$-receptor–mediated synaptic connections were simulated, not *N*-methyl-D-asparatate (NMDA)- or $GABA_B$-receptor–mediated actions. The general form of a unitary e $\rightarrow$ e synaptic conductance was $c_{e\rightarrow e}\, t \exp(-t/2)$, where t is the time in milliseconds and $c_{e\rightarrow e}$ is a scaling parameter; for a unitary e $\rightarrow$ i synaptic conductance, it was $c_{e\rightarrow i}\, t \exp(-t)$. The general form of a unitary IPSP was $c_{i\rightarrow e} \exp(-t/10)$ or $c_{i\rightarrow i} \exp(-t/10)$, respectively. Default values (in RESULTS they are often referred to as "usual" values, because these are the values used in former publications) of $c_{i\rightarrow e}$ and $c_{i\rightarrow i}$ were as follows: $c_{i\rightarrow e}$ i-cell $\rightarrow$ pyramidal cell, 1.6 nS, for all types of i-cells; $c_{i\rightarrow i}$ basket cell $\rightarrow$ interneuron, 2.3 nS; and $c_{i\rightarrow i}$ bistratified or o/lm cell $\rightarrow$ interneuron, 0.23 nS. As indicated in the respective paragraphs, $c_{i\rightarrow e}$ and $c_{i\rightarrow i}$ are set in some simulations to higher values. In a few other simulations $c_{i\rightarrow e}$ and $c_{i\rightarrow i}$ are only enhanced if the presynaptic i-cell is a basket cell. The scaling parameters $c_{e\rightarrow e}$ and $c_{e\rightarrow i}$, and in some simulations, $c_{i\rightarrow e}$ and $c_{i\rightarrow i}$, depend on "learning" in a manner described below.

STIMULATION CONDITIONS. As in Traub et al. (1999), oscillations were evoked by applying tonic "metabotropic" conductances to dendrites of principal cells and interneurons (Whittington et al. 1997a). The reversal potential of this conductance was 60 mV positive to resting potentials. Interneurons received a tonic conductance of 4.0–4.2 nS; pyramidal cells received a maximum tonic conductance of 75.0–82.5 nS. The tonic excitatory conductance to pyramidal cells was time-dependent, starting at 0 at time 0, rising to its maximum over 100 ms (Whittington et al. 1997a), staying constant for the next 700 ms, and then declining linearly with time to 55% of the maximum value, agreeing qualitatively with experimental data (Whittington et al. 1997a).

K^+-AHP AND M-CURRENT CONDUCTANCES. Unlike Traub et al. (1999) and Bibbig et al. (2001), $g_{K(M)}$ and $g_{K(AHP)}$ were kept constant throughout all simulations with a scaling constant of 0.25. Even though experimental data indicate their tetanus-induced time-dependent variation (Whittington et al. 1997b), this was done to concentrate on i $\rightarrow$ e conductance variations and isolate the resulting effects which might be similar to effects of varying $g_{K(M)}$ and $g_{K(AHP)}$. Note that it is conductance *amplitude* that is manipulated in our simulations, but it is *duration* that is of greatest functional importance.

As $[Ca^{2+}]_i$ provides important parameters for our Hebbian learning rule, $[Ca^{2+}]_i$ dynamics in these model neurons should be explained thoroughly: $[Ca^{2+}]_i$ follows a simple first-order kinetic scheme, with updating of the variables every 0.25 ms (i.e., every 100 integration steps). Thus in each compartment, expressing concentration in arbitrary units

$$d[Ca^{2+}]_i/dt = \text{scaling constant} \times I_{Ca} - [Ca^{2+}]_i/\tau_{Ca} \quad (1)$$

In dendritic compartments, we used a time constant τ_{Ca} of 20 ms (Miyakawa et al. 1992; Sabatini et al. 2002) and call it "τ_{post}." To simulate $[Ca^{2+}]_i$ generated by presynaptic activity, a similar scheme was used simulating something like the synaptically mediated component of spine $[Ca^{2+}]_i$ when the postsynaptic cell was a pyramidal cell, although spines were not simulated explicitly. The presynaptic time constant was τ_{Ca} = "τ_{pre}" = 25 ms (Koester and Sakmann 1998). Note that the model does not explicitly simulate the effects of metabotropic glutamate receptors—acting via second messenger pathways—on $[Ca^{2+}]_i$ (Nakamura et al. 1999, 2000; Pozzo-Miller et al. 2000) but simulates only voltage-dependent effects.

"LEARNING." As mentioned at the beginning of METHODS, e → e synapses, e → i synapses, and in simulations shown in Fig. 8, i → e synapses, are modifiable during the course of a simulated oscillation. In general, these synapses modify according to a Hebbian learning rule, in the sense of depending on correlations between pre- and postsynaptic activity. Modification is governed by the following rules.

1. $c_{e\to e}$, $c_{e\to i}$, and $c_{i\to e}$, the scaling constants for e → e, e → i and i → e synaptic connections, respectively, can assume independent values at each synaptic connection, not depending on values assumed at other connections (apart from the initial conditions).
2. The program sets initial values and maximum values for the scaling constants. The minimum values are 0. Initial values are as follows: $c_{e\to e}$ = 0.3 nS; $c_{e\to i}$ = 1.0 nS; and $c_{i\to e}$ = 1.6 nS. Maximum values are as follows: $c_{e\to e}$ = 7.5 nS; $c_{e\to i}$ = 3.0 nS; and $c_{i\to e}$ = 4.8, 8.0, or 32 nS, depending on the simulation.
3. The signals used to "integrate" pre- and postsynaptic activity—and hence used to determine whether synaptic conductances increase, decrease, or remain fixed over some time interval—are $[Ca^{2+}]_i$ concentrations. The "presynaptic" signal can be thought of as a local $[Ca^{2+}]_i$ signal gated by a presynaptic action potential and might correspond (in the case of a pyramidal cell) to the $[Ca^{2+}]_i$ rise in the spine induced by presynaptic activity. The "postsynaptic" signal can be thought of as a localized $[Ca^{2+}]_i$ signal induced by voltage-dependent activity in the postsynaptic cell, in basal dendrites (for pyramidal cells) or selected portions of the dendrites (for interneurons). *Equation 1* shows how $[Ca^{2+}]_i$ dynamics are calculated. The postsynaptic signal used was not $[Ca^{2+}]_i$ in the individual dendritic compartment on which the synapse was located; rather, the total value of $[Ca^{2+}]_i$ was used, summing over compartments on which excitatory synapses could be located. This spatial averaging was done to smooth over wide differences in peak $[Ca^{2+}]_i$ values that could occur at different dendritic locations: consideration of each separate $[Ca^{2+}]_i$ signal would have introduced impractically many parameters into the system, because each dendritic compartment might, in principle, have needed its own values of the learning thresholds. In addition, it should be noted that somatic action potentials propagated, in our model, to all compartments in the basal dendrites with little decrement. We did not explicitly simulate the release of $[Ca^{2+}]_i$ from internal stores, nor the actions of metabotropic glutamate receptors on $[Ca^{2+}]_i$ dynamics.
4. Learning began 175 ms into the simulation to allow equilibration of the system.
5. The learning code was executed once per millisecond. It used a 2-threshold rule formally similar to (but not identical to) that employed by other authors (e.g., Artola et al. 1990; Bienenstock et al. 1982). Thus fixed "postsynaptic" and "presynaptic" thresholds were set at the beginning of the program, T_{post} and T_{pre}, equal to 75 and 1.0, respectively (arbitrary units). If both presynaptically gated and postsynaptic $[Ca^{2+}]_i$ signals were above their respective threshold values, then the appropriate scaling constant was increased by a preset "up" value. If one of the $[Ca^{2+}]_i$ signals was above its respective threshold, but not the other, then the appropriate scaling constant was decreased by a preset "down" value. If both $[Ca^{2+}]_i$ signals were below the respective thresholds, then the scaling constant was not changed (Fig. 1*B*). Specific choices for "up" and "down" values were as follows: $c_{e\to e}$ "up," 18.75 pS; $c_{e\to e}$ "down," 1.875 pS; $c_{e\to i}$ "up," 6.0 pS; $c_{e\to i}$ "down," 0.6 pS, $c_{i\to e}$ "up," 16.00 pS; and $c_{i\to e}$ "down," 1.6 pS.

The reader should note the axonal conduction delays in the system, which are 10 ms and above. It is the correlation between $[Ca^{2+}]_i$ signals at postsynaptic dendrites and *presynaptic terminals* (not presynaptic cell bodies) that control synaptic plasticity, both in the model and also in the real biological system; with such long axonal conduction delays, depolarization at the presynaptic terminal can be delayed by more than one-half of a γ cycle from the action potential at the presynaptic *soma.*

AXON CONDUCTION DELAYS. Pyramidal cell axons conducted at 0.5 mm/ms, and interneuron axons conducted at 0.2 mm/ms. Thus if the minimum conduction delay for excitation between the two blocks shown in Fig. 1 were 10 ms, then the maximum conduction delay would be 13.84 ms, and the average conduction delay was approximately 12 ms. These values were typical, but in the simulation shown in Fig. 4, *C* and *D*, the minimum conduction delay was 15 ms. In analyzing how cells of one site can influence cells of the other site, it must be taken into account that there is a spike generation time: This time *very* much depends on the condition of the cell, the size and form of the excitatory postsynaptic potential (EPSP), and where on the dendrite the EPSP is generated; this can be as short as a fraction of a millisecond and up to many milliseconds. On average it is approximately 2 ms.

NOISE. Noise was simulated, as before (Traub et al. 1999), with ectopic spontaneous axonal action potentials, originated by independent Poisson processes, with an average interval of 10 s in e-cell axons and of 5 s in i-cell axons.

SIGNALS SAVED AND DATA ANALYSIS. The program saved voltages of selected cells (soma, dendrites, terminal axon), $[Ca^{2+}]_i$ signals, and synaptic input conductances. It saved, in addition, e-cell spatial averages (56 cell somata) and i-cell spatial averages (28 cell somata), one average from either end of the array. The average signals are presented both as raw data and in auto- and cross-correlations, the latter using 200 ms of data. Average values of synaptic scaling constants, $c_{e\to e}$, $c_{e\to i}$, and $c_{i\to e}$, were also saved.

DATABASE, RUN TIMES, PROGRAMMING, AND SYSTEMS ASPECTS. More than 70 simulations were performed with the large, detailed model with different e → e, e → i, and i → e conductances, different axonal conduction delays, plasticity at different synapses, etc. Code was written in FORTRAN augmented with extra instructions for a parallel computer and run on an IBM SP2 machine with 12 processors. A typical 2-s simulation took about 6 h to run. For details on programming aspects, contact roger.traub@downstate.edu.

Simple network model

OVERVIEW OF NETWORK STRUCTURE, NEURONAL PROPERTIES, SYNAPTIC CONNECTIVITY, PLASTICITY AND STIMULATION PARAMETERS. Figure 2*A* shows a block diagram of the network structure of the simple model consisting of 120 excitatory neurons (e-cells) and 120 inhibitory cells (i-cells), each modeled as a leaky integrate-and-fire neuron with refractory period and noise term. e-Cells and related i-cells are organized in two chains, which were subdivided into four assemblies of 30 cells each. Usually, assemblies 1 and 3 were stimulated together with a tonic input. The goal was to have assemblies 1 and 3 synchronize to form a "global" cell assembly (as was the goal for the 2 assemblies, 1 and 2 in the detailed model; Fig. 2*B*). As with the detailed model, this synchronization could be reached with the help of interneuron plasticity, that is to say, plasticity of e → i and i → e conductances. e-Cell projections are far-reaching; that is, e-cells from assembly 1 project to e-cells and i-cells of all other assemblies (1–4). In contrast, i-cells project only locally; that is to say, i-cells of group 1 can maximally project to e- and i-cells of assembly 2 (as well as assembly 1), but do not project to e- and i-cells of group 3 (which is simultaneously stimulated and should be synchronized with assembly 1; see goal above) and assembly 4. This means that, in the case of the simple network model, the i → e and i → i connectivity is "functionally local," whereas in the detailed model it is not. We chose

this functionally local i-cell connectivity here in the simple model to show that it is not necessary to have some i → e connections projecting to the respective other assembly for the two assemblies to be synchronized (as we had in the simulations with the detailed model shown here). We also conducted simulations with functionally local i-cell connectivity with the detailed model that shows the same result (not shown here): large enough *local* i → e projections, not reaching the other assembly, are sufficient for synchrony to occur (if e → i connections are far reaching; see RESULTS). Action potential transmission of all neurons occurs via distance-dependent axonal conduction delays of 0.5 mm/ms.

DETAILS OF THE NETWORK STRUCTURE. Connection probability of e → e synapses was 0.3 within a radius of 19 neurons (both to the rightward and the leftward site of a given e-cell), and it was 0.1 to all other e-cells. Connection probability of e → i synapses was 0.6 within a radius of 19 neurons of a given e-cell, and it was 0.3 to all other i-cells. The local connection probability of i → e connections was 0.7 within a radius of 13 neurons (to the right and the left side of a given i-cell), and the connection probability of i → i connections was 1.0 within this radius of 13 neurons. Connection probability of i → e and i → i connections was 0 outside this radius of 13 neurons.

The general form of a unitary e → e and e → i synaptic conductance was $c_{e\to e} \exp(-t)$ and $c_{e\to i} \exp(-t)$, where t is the time in milliseconds and $c_{e\to e}$ and $c_{e\to i}$ are the scaling parameters. The general form of a unitary inhibitory postsynaptic current (IPSC) was $c_{i\to e} \exp(-t/10)$ or $c_{i\to i} \exp(-t/10)$, respectively. Default values, or if the respective synapses are plastic, initial values were as follows: $c_{e\to e} = 0.04$, $c_{e\to i} = 0.05$, $c_{i\to e} = 0.01$, and $c_{i\to i} = 0.01$.

LEARNING RULE. At all synapses (e → e, e → i, i → e, and sometimes i → i) we used a Hebbian two-threshold learning rule (Artola et al. 1990; Bienenstock et al. 1982) with the product of a presynaptic, or more precisely, presynaptically induced signal (EPSP or IPSP) and the postsynaptic signal (spike rate) as a measure (Fig. 2*B*). The product of both signals should approximately represent the intracellular $[Ca^{2+}]$ of a postsynaptic neuron at a real synapse. It should also reflect pre- *and* postsynaptic effects at all these synapses, e.g., the supralinear effects of the EPSP and the postsynaptic back-propagating action potential on $[Ca^{2+}]$ values at e → e synapses (Yuste and Denk 1995), the dependency on presynaptic activation and postsynaptic depolarization at e → i synapses (Perez et al. 2001), and pre- and postsynaptic activity influencing long-term changes at i → e synapses (Holmgren and Zilberter 2001). If the product exceeded the LTD-threshold (long-term depression), the synaptic scaling parameter was decreased by a small amount (Δ). If it was above the LTP threshold (long-term potentiation), this scaling parameter was increased by 5Δ (e → e) or by about 2Δ (e → i and i → e). This learning algorithm was performed every time-step of the simulation, i.e., twice per millisecond.

Programs were written in C, and neuronal network activity could be observed on-line using a neuronal simulator developed by Thomas Wennekers, formerly at the University of Ulm, Ulm, Germany. For details on programming aspects, please contact andrea.bibbig@downstate.edu.

RESULTS

In this paper, we consider patterns of oscillations that involve e-cells and i-cells at two separate regions in neural tissue. Only a finite number of patterns occur in our simulations. It is therefore possible to give each pattern a name (Fig. 3): with short delays (<8 ms), we can get a synchronous γ (Fig. 3*Aa*), a γ oscillation with a phase-shift between the two sites (*Ab*), a synchonous β (*Ac*), and a β oscillation with a large (almost anti-phase) phase-lag between the two sites (*Ad*). With long conduction delays between the two sites (≥8 ms), a synchronous γ oscillation generated by network interactions between the two sites seems impossible (we will argue in Fig. 7 why). However, we can generate a γ oscillation with a large, almost anti-phase phase-shift between the two sites (*Bb*), a synchonous "β" (*Bc*), and a slow oscillation at β or even α frequency with a large (almost anti-phase) phase-lag between the two sites (*Bd*). ("β", because it shares some characteristics with the β oscillations generated with short delays, i.e., β frequency and beat skipping activity of e-cells, whereas i-cells fire at γ frequency; but lacking other characteristics, such as dependence on e → e synapses.) In this paper, we will concentrate on simulations with long axonal conduction delays between the two assemblies, i.e., Fig. 3*B*.

During these oscillations, in each period, e-cells (respectively, i-cells) fire in approximate synchrony with nearby e-cells (respectively, i-cells), or else are silent. In addition, in all the cases we consider, e-cell populations at the two sites fire at nearly the same frequency; likewise, i-cell populations at the two sites fire at nearly the same frequency. (i-Cells, however, may have a different mean frequency than e-cells.) Finally (in almost all cases), e-cells fire 0 or 1 action potentials per period (wave) while i-cells fire 0, 1, or 2 spikes during this time interval. A beat is a population spike of both e- and i-cells, and an e-cell beat (respectively, i-cell beat) is a population spike of the e-cell (i-cell) population. A doublet (or synonymously i-cell doublet or i-doublet) consists of two i-cell action potentials per i-wave, which follow each other in close succession (≤5 ms). With tetanic two-site stimulation and short conduction delays (1–3 ms between the two assemblies), the first action potential of the doublet is generated by tonic input combined with synaptic excitation from local e-cells, whereas the second action potential is generated mainly by the distant e-cells and thus follows the first one after approximate "delay milliseconds" (Traub et al. 1999).

We generalize this idea to larger conduction delays using the term *long-interval doublet* to refer to a pair of interneuron action potentials, also temporally separated by approximately "delay milliseconds" (which can be a large portion of the oscillation period when the two regions are, as in this paper, separated by a delay ≥8 ms). Long-interval doublets are generated by the following two principles: *1*) the first action potential is induced by tonic input and excitation from nearby e-cells, while *2*) the second action potential is induced by (delayed) excitation from distant e-cells. *Long-interval population doublets* are long-interval doublets in all or almost all i-cells of the population. The second beat of an interneuron long-interval population doublet can then inhibit nearby e-cells (which would be expected to fire *after* the i-cell beat assuming inhibition in e-cells is larger/longer than in i-cells; see Figs. 6 and 7). This leads to a firing pattern characterized by e-cells firing on every second period of the underlying i-cell rhythm (i.e., they skip alternate beats; e.g., Fig. 3*Bc*). This means that in oscillations with skipped e-cell beats and long-interval doublets/long-interval population doublets, i-cells generate two action potentials per e-cell period but only one action potential per i-cell period. Long-interval doublets thus do not look like doublets, as previously defined for short inter-areal delays (Traub et al. 1996), but they share a common underlying mechanism.

Summarizing the last paragraphs, oscillation patterns are defined by the following parameters: *1*) frequency of the e-cells

(e.g., $\gamma = 30–70$ Hz, $\beta = 10–29$ Hz); *2*) frequency of the i-cells; *3*) phase angle of the e-cells at one site relative to e-cells at the other site; *4*) phase angles of e-cells at one site relative to i-cells of that site (phase angles—plural—because i-cells may fire more times per cycle than e-cells); *5*) firing pattern of i-cells, e.g., whether or not doublets occur; and *6*) wave-to-wave variations in the number of cells at each site firing per beat. Figure 3 illustrates examples of different oscillation patterns, with references to the literature for those patterns that have been observed experimentally.

The main goal of this paper is to formulate conditions under which two assemblies separated by large conduction delays (10 ms and more—a delay easily reached between neurons in the neocortex) can fire synchronously, either from the beginning of the oscillation or after synaptic plasticity has taken place. The conduction delay value of 10 ms is based on the following experimental data: *1*) axonal conduction velocity is <5 m/s (Swadlow 2000), and *2*) synchrony is observed over distances of ≤ 5 or even 9 cm (Desmedt and Tomberg 1994; Tallon-Baudry et al. 2001). Even if areas separated by distances of several centimeters are likely to be connected by relatively fast cortico-cortical connection (although the relevant axonal conduction delays are not known), there are axonal collaterals within the gray matter reported to conduct with axonal conduction velocities as small as 0.1 mm/ms (Aroniadou and Keller 1993). Thus even spatial separations of 3–4 mm (common for extrinsic collaterals; Rockland and Drash 1996), or of 3–6 mm (common for intrinsic, i.e., within-area, collaterals; K. Rockland, personal communication) lead to large temporal separations, in principle up to 60 ms. Thus a 10-ms delay seems quite plausible. As synchronization has been reported over these distances, there must be a mechanism for synchronizing neocortical neuronal assemblies despite significant separation in space and/or very large conduction delays. A further comment on terminology: If we use terms like initial synchrony or capability of developing synchrony, we are interested, respectively, in whether or not the two assemblies fire synchronously from the beginning of the oscillation or whether

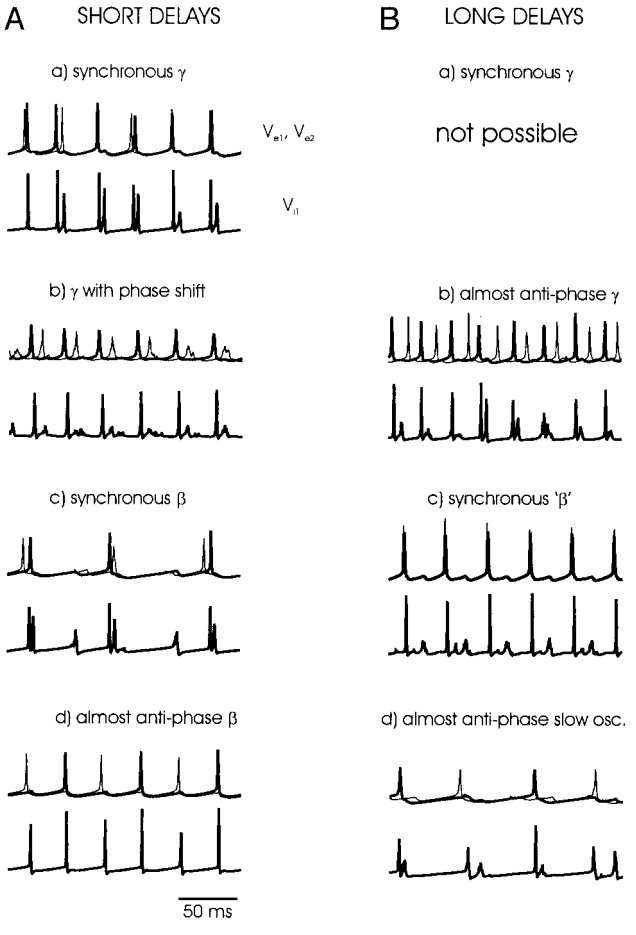

FIG. 3. Examples of oscillation patterns found in detailed network simulations modeling 2 assemblies (each comprising e-cells and i-cells) separated by short (2 ms average) or long axonal conduction delays (12 ms on average). *Toptraces*: average e-cell voltages from either end of the array [designated here as V_{e1} (thick line) and V_{e2} (thin line)], for left and right, respectively. *Bottom trace*: average i-cell voltage from the first site (V_{i1}). The time scale bar is the same for all recordings. *A*: different oscillation types found with short axonal conduction delays between the 2 assemblies. *Aa*: synchronous oscillation at γ frequency (usually 40–50 Hz in the simulations with the detailed and the simple network model, i.e., 20- to 25-ms period). In this type of oscillation the e-cells of the 2 assemblies fire almost synchronously (V_{e1}, V_{e2}), with an average phase lag of less then 2 ms between the 2 sites. The i-cells generate 2 spikes most of the time, i.e., they fire doublets, which stabilize synchrony between the 2 sites. This type of oscillation is seen, for example, in hippocampal slices stimulated at 2 sites with a tetanic stimulus (Traub et al. 1996; Whittington et al. 1997a). *Ab*: γ frequency oscillation with a phase-lag between the 2 sites. Here (most of) the i-cells only generate 1 spike/wave, seen in the *bottom trace*, showing the average i-cell signal of assembly 1. This kind of oscillation is seen in hippocampal slices if 2 sites are stimulated simultaneously after only 1 site was stimulated strongly before (Bibbig et al. 2001; Whittington et al. 1997b). *Ac*: synchronous oscillation at β frequency (usually 10–25 Hz, i.e., 40- to 100-ms period in simulations). Here, the 2 e-cell assemblies fire (almost) synchronously during the so-called strong beats (3 of them are shown in the *top* e-cell traces), whereas they do not fire in between in the 2 missed beats in the middle, where only i-cells are active (see *bottom trace*). Due to longer-lasting e-cell afterhyperpolarizations (AHPs; compared with i-cell AHPs), the i-cells actually fire just before the e-cells would fire their next beat, and thus inhibit the e-cells so that the e-cell beat is skipped. Note that the i-cells fire doublets during the strong beats and only singlets during the missed beats due to the lack of e-cell input, so that only the tonic input is available. Synchronous β is seen in hippocampal slices after a strong tetanic 2-site stimulation (Traub et al. 1999; Whittington et al. 1997b). *Ad*: almost anti-phase β oscillation. Here the 2 e-cell assemblies fire alternately and the i-cells only generate singlets. (Nearly) anti-phase β is sometimes experimentally observed with tetanic 2-site stimulation in the presence of diazepam (Faulkner et al. 1999). *B*: different oscillation patterns found with long axonal conduction delays between the 2 assemblies. Because there are no slices available with average axonal conduction delays this large, only oscillation types found in simulations are mentioned. These types of oscillations might, however, occur in vivo. *Ba*: synchronous oscillations at γ frequency are not seen in simulations with detailed or simple models if the 2 assemblies are separated by long axonal conduction delays (Bibbig 2000; Kopell et al. 2000). *Bb*: almost anti-phase γ frequency oscillation. Here the i-cells more often generate singlets than they generate doublets, although in every beat some i-cells do generate a doublet (seen as second small "population spike" in the average i-cell trace of the first assembly; see e.g., Fig. 7). *Bc*: synchronous oscillation at β frequency (usually approximately 20–30 Hz, i.e., 35- to 50-ms period in simulations). This "β" has different characteristics than have β oscillations with short conduction delays (see Fig. 8). Note that Tallon-Baudry et al. (2001), in human memory tasks, only record γ oscillations that are not synchronized between the 2 areas (separated by several centimeters, the conduction delay not being directly accessible in humans), whereas, in contrast, β oscillations are synchronous. This is consistent with our simulations shown in Fig. 3*B*, *a–c*. *Bd*: almost anti-phase slow oscillation (usually approximately 7–10 Hz, 100–130 ms), i.e., the frequency is low, in the θ or α range. The oscillation is almost anti-phase, and like β oscillations, shows strong and missed e-cell beats. In addition, the missed e-cell beats here are not synchronous but come with a phase lag of approximately "delay + spike generation time" milliseconds after the strong beat of the respective other site. Remark: similar oscillations as shown in Fig. 3, *A* and *B*, can also be obtained with the simple network model.

or not the two assemblies are able to synchronize their activity after some period of time dependent on characteristics of plasticity.

In all simulations with the detailed network model shown in this paper, if not explicitly mentioned otherwise, e → e and e → i conductances were plastic according to a Hebbian learning rule, which takes two [Ca^{2+}] values as measures (see Methods and Bibbig 2001): *1*) [Ca^{2+}] fluctuations induced by presynaptic activity and *2*) [Ca^{2+}] signals induced by postsynaptic voltage-dependent g_{Ca}. In simulations with the simple network model, these two kinds of synapses (e → e and e → i) were also plastic following a Hebbian learning rule, dependent on the EPSP (as a presynaptically induced measure) and postsynaptic instantaneous firing rate. We made numerous further simulations to show that plasticity of the e → e and e → i conductances per se is not essential for synchrony. That is, we could have shown instead nonplastic simulations, with certain fixed values for the e → e and e → i conductances; such nonplastic networks can also generate synchronous oscillations, exhibiting the same parameter-dependences, for synchronization of two assemblies separated by large conduction delays, as the plastic networks shown here in this paper. We chose, however, to show simulations with plastic e → e and e → i conductances, because there are experimental data demonstrating that these synapses are indeed plastic during tetanus-induced γ oscillations: in vitro experiments using tetanic stimulation to yield synaptic potentiation or depression (Bibbig et al. 2001; Whittington et al. 1997b). In addition, there are other experimental data about e → e and e → i plasticity under different experimental conditions (see e.g., Geiger et al. 1999 for a review of e → i plasticity). In vivo, there are experiments in freely moving rats, where stimulation of the perforant path with LTP- or LTD-inducing tetanic stimuli leads to changes in the network behavior of CA1 pyramidal cells, suggesting that plasticity at least of e → e synapses plays a role there (Dragoi et al. 2000) and should be considered in our models.

In former papers we have shown the effect of growing e-cell AHPs on $\gamma \rightarrow \beta$ oscillations (Traub et al. 1999; Whittington et al. 1997b). However, it has now been shown that i → e conductances also grow during γ frequency activity induced by tetanic or theta-patterned stimulation (see Jensen et al. 1999 for short-term effects and Chapman et al. 1999; Grunze et al. 1996; Perez et al. 1999 for long-term potentiation). i → e Conductances also appear to grow by approximately a factor of two during tetanically induced two-site $\gamma \rightarrow \beta$ oscillations (Whittington, unpublished data). To elucidate a possible site for synaptic plasticity in these oscillations, we removed any changes of the intrinsic e-cell AHP and concentrated on the plasticity of i → e conductances. This does not mean that we believe AHPs do not play a role in synchronizing two assemblies separated by large conduction delays. Rather, it means that i → e conductances can, in principle, do the job. This is important to know, because there are, to our knowledge, no experimental data on synchronizing mechanisms with such long delays available yet.

One of the major issues of this paper will be the dependence of synchrony of two assemblies separated by large conduction delays on the i → e conductance. We first examine how synchrony changes with the variation of a fixed i → e conductance (Fig. 4, *A* and *B*, *C* and *D*). Then we further analyze, for a given fixed i → e conductance, how the synchrony behavior changes with other parameters such as delay (Fig. 4, *B* and *C*) or i → i conductance (Fig. 5), and we try to explain how and under which conditions the two assemblies fire in-phase (Figs. 6 and 7), or develop an almost anti-phase oscillation (Fig. 7). Later on (starting in Fig. 8), we shall use plastic i → e synapses to examine under which conditions two formerly asynchronous firing assemblies are able to synchronize their activity.

Synchrony may be possible with larger conduction delays, if basket cell → pyramidal cell conductances are large enough.

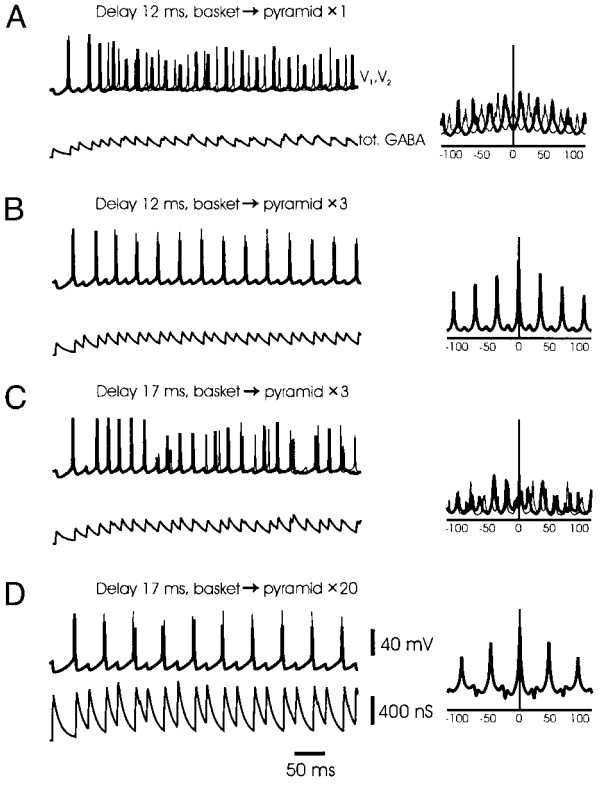

FIG. 4. Whether 2 assemblies separated by large conduction delays are able to synchronize depends on the delay and on the basket cell → pyramidal cell conductance. *Left traces*: average e-cell voltages from either end of the array [designated here as V_1 (thin line) and V_2 (thick line)] and the total $GABA_A$ conductance received by a single e-cell at the first site, respectively. Voltage traces and $GABA_A$ conductances show 500-ms runs. *Right traces*: auto- (thin line) and cross-correlations (thick line) of the 200-ms interval [300 ms, 500 ms] of V_1 and V_2, respectively. Scale bars are the same for all voltage traces, total $GABA_A$ conductances, and time in *A–D*. *A*: case with an average conduction delay of 12 ms between the 2 assemblies and the usual (fixed) basket cell → pyramidal cell conductance (see METHODS). The 2 sites are not able to synchronize, but stabilize in an almost anti-phase oscillation, as seen in the voltage traces and the cross-correlogram (oscillation period: 25.7 ms). *B*: increase of the fixed basket cell → pyramidal cell conductance by a factor of 3 synchronizes the 2 assemblies (again separated by 12 ms on average), from the beginning of the oscillation (oscillation period: 36 ms). As described in METHODS, there are 4 different kinds of i-cells: basket cells, axo-axonic cells, bistratified cells, and o/lm-cells. The synaptic coefficients are $c_{i \rightarrow e} = 1.6$ nS (see METHODS). Because only the basket cell → e-cell conductance is enhanced to 3 times the usual value and not all the other i → e conductances, the total i → e conductance is only enhanced by a factor of 1.5, an elevation that is hardly seen in the trace of the "*total* $GABA_A$ conductance received by a single e-cell" shown here, but it is measurable. *C*: increase of the average delay from 12 to 17 ms again makes the synchrony disappear, if the same basket cell → pyramidal cell conductance is used as in *B*. Voltage traces V_1 and V_2 and the cross-correlation show poorly correlated activity (peak of the auto-correlogram at 23.1 ms). *D*: the 2 assemblies synchronize despite the large average delay of 17 ms, following a further increase of the basket cell → pyramidal cell conductance to 20 times the usual value (see METHODS), with an oscillation period of 48 ms.

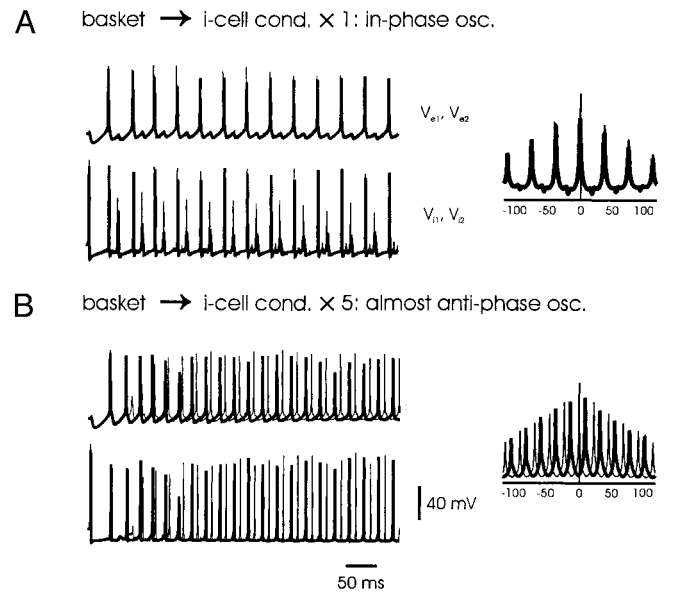

FIG. 5. For a given i → e (more precisely, basket cell → e-cell) conductance the synchrony depends on the i → i conductance. *Left traces*: 500 ms of the average e-cell voltages from either end of the array [*top traces*: designated as V_{e1} (thin line) and V_{e2} (thick line)] and the same time span of the average i-cell averages from the respective sides (V_{i1}, V_{i2}). *Right traces*: auto- (thin line) and cross-correlations (thick line) of the interval [300 ms, 500 ms] of V_1 and V_2. Scale bars are the same for all voltage traces and time scales in *A* and *B*. *A*: simulation of 2 assemblies separated by an average delay of 12 ms and a basket cell → e-cell conductance of 5 times the "usual" value. The i → i conductance was at its usual value (used in all simulations with the detailed model shown here other than *B*). The 2 assemblies fire synchronously with an oscillation period of 38 ms. Note that the i-cells fire twice during an e-cell oscillation period, i.e., they fire long-interval population doublets (please see Fig. 6 for explanation). *B*: another simulation of 2 assemblies separated by an average delay of 12 ms and a basket cell → e-cell conductance of 5 times the "usual" value, but this time the i → i conductance was also increased to 5 times the "usual" value. Now the two assemblies stabilize in an almost anti-phase oscillation with 1 site leading the other by 10.3 ms, as most clearly seen in the cross-correlogram of the last 200 ms of the voltage traces. The oscillation is at γ frequency with a period of 23 ms. Note that the i-cells here only fire once per e-cell oscillation period.

Two synchronously firing assemblies separated by >8-ms fire with a characteristic pattern: i-cells fire at γ frequency, whereas e-cells only fire every other beat (i.e., they skip every second beat) and thus fire at β frequency! Two sites, separated by a conduction delay of 12 ms on average, stabilize their firing pattern in an oscillation with a fixed phase angle of almost one-half the oscillation period at γ frequency (period, 26 ms; Fig. 4*A*). This almost anti-phase oscillation occurs in a simulation where all synaptic conductances and AHPs take on their default or usual values (i.e., the values used in former publications, e.g., Traub et al. 1999; see also METHODS). Two assemblies separated by short delays (e.g., 2 ms and other delays ≤6 ms) would fire synchronously with the same parameters (see e.g., Fig. 4 of Traub et al. 1999 and Fig. 3 of Bibbig et al. 2001 for simulations with short conduction delays and other parameter values similar to the ones used here). If the basket cell → pyramidal cell conductance is multiplied by a factor of three, leaving all other parameters unchanged, then the two sites are able to fire synchronously in an oscillation at β frequency (oscillation period: 36 ms), exhibiting missed e-cell beats. This synchrony occurs despite an average conduction delay of 12 ms (Fig. 4*B*).

A further increase of the conduction delay between the two assemblies (from 12 to 17 ms), with all other parameters unchanged, generates an oscillation that is barely correlated, with changing phase shifts from period to period and with a γ peak in the auto-correlogram at 23.1 ms (Fig. 4*C*). Yet, with a still further increase of the basket cell → pyramidal cell conductance to 20 times the usual value (see METHODS), the two assemblies can synchronize, despite their separation by a large average delay of 17 ms (Fig. 4*D*). The oscillation period is now 48 ms, i.e., in the β frequency range. An elevation to 10 times the usual value was not sufficient for synchrony to occur (not shown); values between 10 and 20 were not tested. The reader should remember that i → e synaptic conductances and AHPs have similar effects on synchronization. Furthermore, the AHP is *not* being enlarged in these simulations (to focus on effects of i → e synaptic conductance variations), so although 20 seems to be a very large factor, the factor would be considerably less if long-duration AHPs were also included. How much less the factor would be depends on an analysis of the respective amplitudes and time courses of IPSCs and AHPs and is beyond the scope of this paper.

In summary, these data show that sufficiently large basket cell → pyramidal cell conductances can synchronize two assemblies at a given delay, in cases when smaller basket cell → pyramidal cell conductances cannot provide such synchrony. Figure 4 further indicates that the larger the delay between the two assemblies is, the higher must be the necessary basket cell → pyramidal cell conductance for synchronizing them. Numerous other simulations were consistent with these notions using both the detailed network model and also using the simple network model (see METHODS) in which only one type of i-cells exist (data not shown). The above statements also appear to be true for several plasticity conditions (data not shown), including networks without any plasticity, networks with only e → e plasticity, and networks with both e → e and e → i plasticity. If some of the synapses are not plastic, i.e., their conductances cannot potentiate during the simulations, they have to be set to certain high fixed values.

A further important point to be made: increasing the basket cell → pyramidal cell or overall i → e conductances had no desynchronizing effects on the synchrony behavior of two assemblies separated by short delays; thus if the assemblies fired synchronously with smaller basket cell → pyramidal cell or i → e conductances, then they continued to fire synchronously with the enlarged conductances. That is, larger basket cell → pyramidal cell or i → e conductances really do enlarge the area, over which two assemblies can synchronize. We will show the reason for this in Figs. 6 and 7.

For a given i → e conductance (and a given delay), the ability to fire synchronously at β frequency, in contrast to firing in an almost anti-phase or hardly correlated γ oscillation, depends in part on the i → i conductance. Figure 5*A* shows a simulation of two assemblies separated by an average conduction delay of 12 ms and a basket cell → e-cell conductance of five times the usual value (see METHODS). Here, the i → i conductance was at its usual value. With these parameters, the two assemblies fire synchronously with an oscillation period of 38 ms, i.e., at β frequency. This is expected, given that two assemblies separated by an average delay of 12 ms could synchronize with a basket cell → e-cell conductance of only three times the usual value (Fig. 4*B*). Figure 5*B* shows again a

simulation of two assemblies separated by an average delay of 12 ms, and a basket cell → e-cell conductance of five times the usual value, but this time, in addition, the i → i conductance was enhanced to five times its usual value. This generates an oscillation in which the two assemblies start in phase, but progressively change to fire with a fixed phase angle with one site leading the other by approximately "delay milliseconds," at γ frequency with an oscillation period of 23 ms, i.e., they fire almost in anti-phase. Note that, in the synchronous oscillation shown in Fig. 5*A*, the i-cells produce two spikes per oscillation period of the e-cells, whereas they only fire once per period in the almost anti-phase oscillation shown in Fig. 5*B* (see Figs. 6 and 7 for explanation). Many other simulations were consistent with this observation (see for example the one shown in Fig. 7*B*). We also obtained a similar result when only the basket cell → i-cell conductance (and not the i → i conductance of all 3 types of possible presynaptic i-cells) was enhanced by a factor of five (data not shown). In addition, these results were

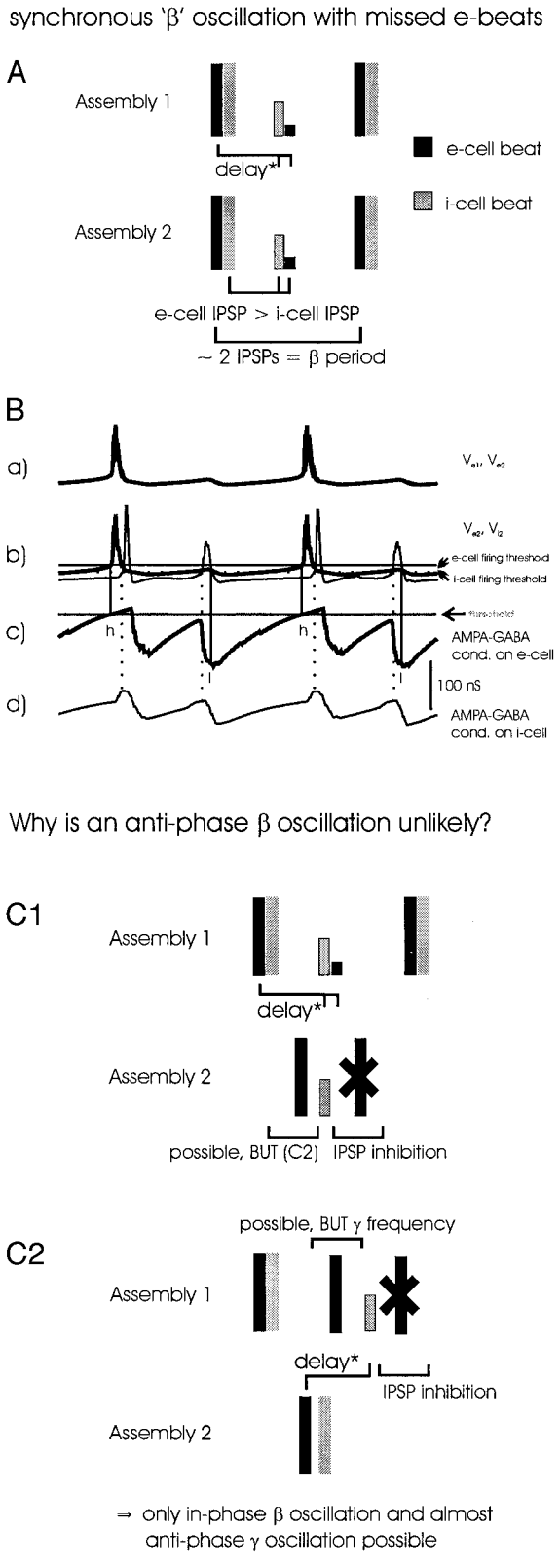

FIG. 6. *A*: 2 assemblies separated by a large conduction delay can fire synchronously at β frequency—with skipping of alternate e-beats under the following 2 conditions: (a) e-cells of assembly 2 are still inhibited when activation from assembly 1 e-cells reaches i-cells (and e-cells) of assembly 2, i.e., after approximately "delay + spike generation time milliseconds" (indicated here as delay*) and (b) the e-cell IPSP must last longer than the i-cell IPSP, so that assembly 2 e-cells do not fire before assembly 2 i-cells. For similar IPSC time constants, i → e conductance must be larger than i → i conductance. Under these conditions, long-interval population doublets can suppress e-cells on alternate waves (as seen here in the second wave); [β oscillation, because the oscillation is at β frequency, but contrary to a β oscillation with short conduction delays (Traub et al. 1999) is not dependent on e → e synapses.] *B*: simulation confirming the hypotheses of *A*. Shown here are the intervals 160–230 ms of a simulation already shown in Fig. 4*B*. *Top traces*: (*Ba*) are average e-cell voltages from either end of the array (V_{e1} and V_{e2}). *Middle traces*: the average e-cell voltage (V_{e2}, thick line, an identical copy of the *top*) and the average i-cell voltage ($V_{i2,}$ thin line) from one end of the array (*Bb*). *Bottom traces*: "total AMPA conductance minus the basket cell $GABA_A$ conductance onto a particular e-cell" (*Bc*), and onto a particular basket cell (*Bd*), both from the same end of the array as the voltage averages in the *middle trace*. This difference signal provides an estimate of the net excitation to the neuron. Traces in *Ba* show that the two assemblies fire at β frequency with missed e-cell beats, and that they fire almost synchronously. In the traces of *Bb*, one can see that the second beat of the "long-interval population doublet" (generated by the e-cells of the other site represented as the thin line in *Ba*) is generated shortly before the e-cells would reach their spike threshold again (indicated by the solid line). This leads to a drop in the "AMPA -$GABA_A$ conductance" of the e-cells seen in the one depicted e-cell in *Bc*. As a consequence of the high $GABA_A$, equivalently low "AMPA -$GABA_A$" conductance (indicated here by the "l" for "low" in contrast to "h" for "high"), the e-cells cannot fire their next beat, but instead skip it. They are able, however, to fire again at the next later beat, when the e-cell $GABA_A$ conductance is low and the combined "AMPA -$GABA_A$ conductance" is high again (h). Contrary to the e-cells, i-cells are able to fire again when the excitation from the distant site arrives (seen as the little bump in the AMPA-$GABA_A$ conductance on a particular i-cell in *Bd*). Note that the i-cells are more strongly excited (larger, faster rising AMPA-$GABA_A$ conductance) during the strong e-cell beats than during the missed e-cell beats, which leads to a stronger and more synchronized i-cell population activity during these alternating beats. *C*: why are 2 assemblies, which fire at β frequency with missed e-cell beats and conditions (a) and (b) (as is *A*), unlikely to fire in almost anti-phase? *C1*: imagine assembly 1 firing a strong beat that excites some i-cells of assembly 2 after approximately "delay + spike generation time milliseconds" even before e-cells of assembly 2 are activated. Due to the population IPSP generated by this small number of i-cells, the next e-cell beat of assembly 2 cannot be generated just after this weak i-cell beat (as indicated by the cross). The next e-cell beat could, however, be generated just before the i-cell beat (which would then not lead to a weak i-beat as it would activate the rest of the i-cells). *C2*: next step in this scenario, given that the e-cell beat of assembly 2 was generated just before the i-cell beat (which as a consequence is also a strong beat, indicated by its large size). With the same argument as used in *C1*, this e-cell beat generates a weak i-cell beat of assembly 1 after approximately "delay + spike generation time milliseconds" that prohibits any e-cell activity of assembly 1 just after this i-cell beat. Again, as in *C1*, there could be an e-cell beat just before the i-cell beat, but if this argument is continued for some more steps, the period length becomes shorter and shorter leading eventually to γ instead of β frequency.

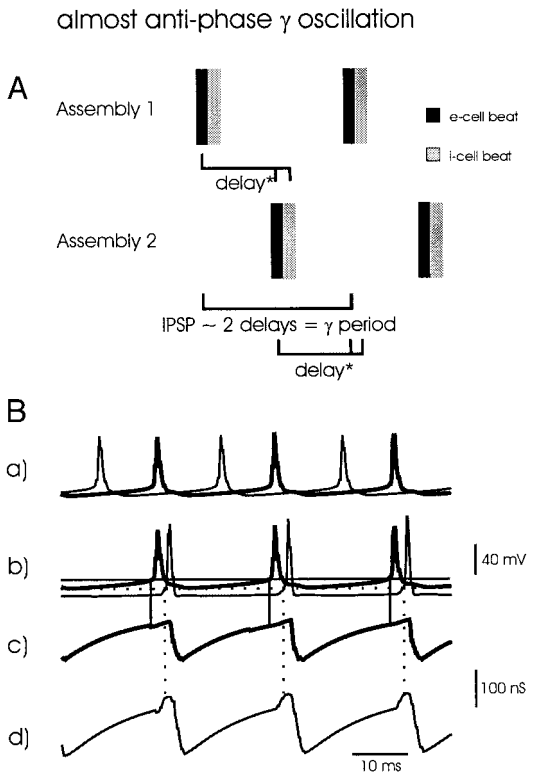

FIG. 7. *A*: two assemblies, separated by a large conduction delay, firing at γ frequency, cannot fire synchronously but only in almost anti-phase. In this case, e-cells of assembly 1 can—after "delay + spike generation time milliseconds" (marked here as delay*)—activate i-cells (and/or e-cells) of assembly 2. Thus both conditions characterizing 2-site γ oscillations are fulfilled: (a) IPSPs that are approximately twice as long as the delay determine the γ period length, and (b) 2-site interactions are possible despite these large conduction delays. An almost anti-phase oscillation is the only possibility for two assemblies separated by $\geq$8 ms to fulfill both (a) and (b). *B*: simulation confirming the reasoning of *A*. Shown here is the interval 160–230 ms of a simulation with an average delay of 12 ms and with a basket cell $\rightarrow$ e-cell conductance and a basket cell $\rightarrow$ i-cell conductance both having 3 times the "usual" values. Average e-cell voltages from either end of the array (V_{e1} and V_{e2}) show an almost anti-phase oscillation at γ frequency (period 22 ms; *Ba*). *Middle traces*: average e-cell voltage (V_{e2}, thick line, an identical copy of the top part) and the average i-cell voltage ($V_{i2,}$ thin line) from one end of the array (*Bb*). They show the absence of "long-interval population doublets" (i.e., in the present case, e-cells fire as often as i-cells and do not skip beats). *Bottom traces*: estimates of net excitatory input: the "total AMPA conductance minus the basket cell $GABA_A$ conductance onto a particular e-cell" (*Bc*), and onto a particular basket cell (*Bd*), both from the same end of the array as the voltage averages in the *middle trace*. This contrasts with the curves seen in Fig. 6*B*, *c* and *d*, in which the smallest "bumps" in the AMPA-$GABA_A$ conductance at a particular i-cell in Fig. 6*Bd* demonstrated the excitatory AMPA input from the other site's e-cells. In Fig. 6*B*, this excitatory input was sufficient to counterbalance the inhibitory $GABA_A$ input and generate the "long-interval population doublet," seen as the two small i-cell population spikes (not accompanied by e-cell population spikes) in Fig. 6*Bb*.

confirmed in simulations using networks of simple neuronal models (data not shown). That fact that too high of an i $\rightarrow$ i conductance makes long-range synchrony impossible is interesting given the fact that, to our knowledge, basket cell $\rightarrow$ i-cell conductance potentiation is not so far described in the experimental literature and might therefore be absent in the brain. As one exception, population IPSPs from one special sort of synapse, namely synapses from stratum oriens-alveus interneurons to other hippocampal interneurons, potentiate during a tetanus-induced γ oscillation, whereas there is no evidence for population IPSP potentiation in other areas, i.e., basket cell $\rightarrow$ i-cell synaptic conductances do not appear to potentiate (Whittington, unpublished data). In contrast, *depression* of i $\rightarrow$ i conductances is reported in rat somatosensory cortex (Tamás et al. 2000).

Figures 4 and 5 suggest that there is a relationship between i $\rightarrow$ e and i $\rightarrow$ i conductances, regarding synchronization of two assemblies separated by large conduction delays: for a given i $\rightarrow$ e conductance, the i $\rightarrow$ i conductance may not be too large, if synchronization is to occur. The same holds for the relationship between the i $\rightarrow$ e conductance and the delay: for a given i $\rightarrow$ e conductance the delay may also not be too large, if synchronization is to occur. In addition, all our simulations with large conduction delays show two assemblies oscillating at β frequency with missed e-cell beats fire synchronously, and, the other way around, synchronously firing assemblies separated by large conduction delays always show a β oscillation with missed e-cell beats (see e.g., Figs. 4, *B* and *D*, and 5*A*). In Fig. 6 we demonstrate that under the conditions mentioned above regarding i $\rightarrow$ e and i $\rightarrow$ i conductances and delay, we get a β oscillation with missed e-cell beats, and show

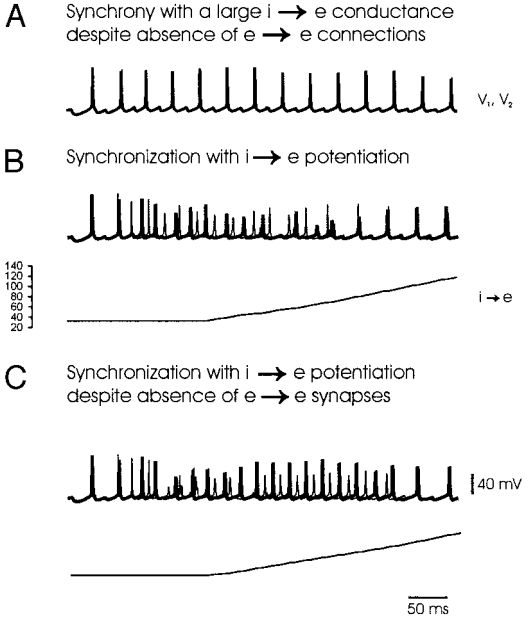

FIG. 8. e $\rightarrow$ e connections are not necessary for synchronization of 2 assemblies separated by large conduction delays and assemblies can synchronize their activity after an almost anti-phase oscillation with the help of interneuron plasticity. *Traces* in *A* and *top traces* in *B* and *C* are average e-cell voltages from either end of the array (V_1 and V_2). *Bottom traces* in *B* and *C* show the average i $\rightarrow$ e conductance (i $\rightarrow$ e). Scale bars are the same for all voltage traces, the i $\rightarrow$ e conductance traces and time scales in *A*–*C*. All traces show the first 500-ms parts of 2-s runs. *A*: 2 assemblies separated by 12 ms on average can fire synchronously with a high fixed basket cell $\rightarrow$ e-cell conductance (3 times the usual value; compare Fig. 3*B* with the same values) even without any e $\rightarrow$ e connections present. *B*: 2 assemblies separated by 12 ms on average and firing asynchronously after 2 synchronous beats in the beginning (basket cell $\rightarrow$ e-cell conductance = "usual" value) can later on synchronize their activity if the "basket cell $\rightarrow$ e-cell conductance" is potentiated. Here, during the first 175 ms, as in all our detailed network simulations, all synaptic conductances (i.e., also e $\rightarrow$ e and e $\rightarrow$ i synapses) were kept constant to let the system organize itself. Then, the synapses began to potentiate with a learning rule similar to the one used for e $\rightarrow$ e and e $\rightarrow$ i synapses, but with low learning thresholds. After an interval of anti-phase activity, the 2 assemblies are able to synchronize their activity. *C*: 2 assemblies can also synchronize their activity by basket cell $\rightarrow$ e-cell potentiation in the absence of any e $\rightarrow$ e synapses in a simulation otherwise identical to *B*.

in a simulation that such an oscillation is indeed synchronous. In Figs. 6*C* and 7 we demonstrate more generally why, with long conduction delays, we either obtain an asynchronous almost anti-phase γ or a synchronous β (i.e., explain Fig. 3*B*,*a*–*c*).

Two assemblies separated by large conduction delays can fire synchronously at β frequency under the following two timing conditions. *a*) e-Cells of assembly 2 are still inhibited "delay + spike generation milliseconds" after the e-cell beat of assembly 1. This means that the e-cell IPSP cannot be significantly shorter than the delay (2-site effect). *b*) The e-cell IPSP must last longer than the i-cell IPSP, i.e., the i $\rightarrow$ e conductance must be sufficiently large and the i $\rightarrow$ i conductance sufficiently small (local effect). As shown in the scheme of Fig. 6*A*, with these two conditions in place the following series of events can happen: *1*) i-cells of site 2 are activated by e-cells of site 1 after approximate "delay + spike generation milliseconds" (symbolized as delay* in Fig. 6), provided that the long-range e $\rightarrow$ i conductance is large enough, and *2*) because of condition *a*), e-cells are still inhibited when i-cells are activated after approximate "delay + spike generation milliseconds," and because of condition *b*), i-cells can themselves be activated. Thus under these conditions, i-cells of site 2 fire *before* the e-cells of the same site. That is, the second beat of a long-interval population doublet can be generated (at site 2 by site 1 excitation) before the site 2 e-cells are ready to fire their next beat. This "next site 2 e-beat" is therefore skipped (due to this inhibition from the local i-cells) and thus an oscillation at β frequency with skipped e-cell beats is generated (marked by the small black square). Thus, although there are some i-cells projecting to e- and i-cells of the distant assembly (see Fig. 1 and METHODS), the critical inhibitory interaction is a local one (contrary to the 2-site e $\rightarrow$ i effect). This was confirmed in additional simulations of networks with functionally local i $\rightarrow$ e and i $\rightarrow$ i connections (see METHODS, results not shown), which had no i-cells projecting to the respective other assembly. We will further argue in the paragraphs describing Fig. 6*C* that an oscillation at β frequency with this pattern cannot be (almost) anti-phase but will be synchronous.

Figure 6*B* shows that the above scheme actually works in simulations: it displays part of a simulation already shown in Fig. 4*B*, i.e., with 12-ms delay, on average, between the two assemblies, and basket cell $\rightarrow$ e-cell conductance three times the usual value. The *top traces* (Fig. 6*Ba*) show that the two assemblies fire at β frequency with missed e-cell beats, and that they fire almost synchronously. The solid horizontal line in Fig. 6*Bb* indicates the approximate threshold of the e-cell population spike. [We here use the total AMPA minus $GABA_A$ conductance as an estimate of cell excitation. Although it omits many important details of synaptic integration in complex multi-compartment neuronal models, the total AMPA minus $GABA_A$ conductance gives a crude measure of the net synaptic excitation a particular neuron receives. Also, as AMPA receptor–mediated excitation is short-lasting relative to inhibition, this signal is roughly equal to minus total $GABA_A$ conductance during the latter part of the oscillation cycle.] Threshold is reached twice during the time course shown (marked by an "h" for high AMPA minus $GABA_A$ conductance) so that the e-cells fire, whereas threshold is missed also twice (indicated as "l" for low), so that the e-cells skip these beats. As seen in Fig. 6*Bb*, the second spike of the long-interval population doublet (generated by the e-cells of assembly 1) is generated shortly before the e-cells would reach their spike threshold again. The phase shift from the peak of the firing of site 1's e-cells to the mentioned second spike of the long-interval population doublet is 14.5 ms, the average delay between the two sites is 12 ms, and the spike generation time is about 2 ms. As a consequence of this i-cell activity, the AMPA minus $GABA_A$ conductance in the e-cells is diminished to a low value (indicated as "l" under the trace of Fig. 6*Bc* showing the total AMPA conductance minus basket cell $GABA_A$ conductance onto one particular e-cell), and the AMPA minus $GABA_A$ conductance threshold of the e-cells (horizontal line in Fig. 6*Bc*) will not be reached; thus the "next beat" is skipped. The e-cells are then able to fire again in the *next* beat, when the AMPA minus $GABA_A$ conductance of the e-cells is high again (h). In summary, this activity pattern again shows an oscillation where e-cells fire at β frequency on every other period of the underlying i-cell γ oscillation, owing to the second set of action potentials in a long-interval population doublet, preventing alternate e-cell firing. This mechanism seems to stabilize an in-phase oscillation: as mentioned before, all of the synchronous oscillations shown in Figs. 4–6*B*, and numerous other simulations not shown here, exhibit this kind of oscillation pattern, and in reverse, all simulations showing this oscillation pattern are synchronous.

We will further analyze, in this paragraph and in Fig. 6*C*, why an oscillation at β frequency with missed e-cell beats can be and will be synchronous, whereas two assemblies separated by long conduction delays firing at γ frequency will exhibit large phase lags and thus fire almost in anti-phase. For this we try to address the question: what are the important characteristics of two assemblies, both containing e- and i-cells, oscillating at γ or β frequency? If there is no common input from somewhere else to pace them, two characteristic features are important: *1*) the population IPSPs, the duration of which determines the period length of the γ oscillation (and roughly one-half of the β period), and *2*) interactions between the two assemblies. With short conduction delays ($\sim$2 ms) between the two assemblies, it is easy to fulfill both conditions in a γ oscillation as interactions between the two sites (e.g., the second beat of an i-cell doublet) can take place within the same beat (Fig. 3*Aa*). With long conduction delays ($\geq$8 ms), however, the only possibility to obtain a γ oscillation with a period length of 20–25 ms (i.e., 40–50 Hz) *and* interactions between the two assemblies is an almost anti-phase oscillation (Fig. 7, *A* and *B*). On the other hand, synchrony can be reached and interactions between the two sites are possible (long-interval population doublets) during a slower β oscillation (Fig. 6*A*).

The above conditions *1*) and *2*), and conditions *a*) and *b*) mentioned in the paragraph about Fig. 6 (introducing relations between i $\rightarrow$ e and i $\rightarrow$ i conductances and delay), also give a heuristic argument of why this β oscillation cannot be (almost) anti-phase (Fig. 6*C*). First of all, as seen in Fig. 6*C1*, assume a strong first beat of assembly 1. This would be followed, after approximate "delay + spike generation time milliseconds" (symbolized by delay*) by a weak i-beat of assembly 2 [*a*) and *b*) will generate the next round of i-cell action potentials of assembly 2 *before* e-cell action potentials are generated in this assembly]. Because of the inhibition following this i-cell beat of assembly 2 and its resulting IPSP, a strong e-cell beat of assembly 2 cannot be generated shortly *after* this i-cell beat.

On the other hand, a strong e-cell beat can also not be generated just *before* this i-beat because of *a*) and *b*). Together, these conclusions imply that almost anti-phase activity at β frequency is not possible with long axonal conduction delays. Even if we assume that the next e-cell beat of assembly 2 (maybe because of jitter) could be generated just before the i-cell beat of assembly 2 (as shown in Fig. 6, *C1* and *C2*), anti-phase β will not persist. As a first consequence, the e-cells of assembly 2 would excite all i-cells of assembly 2, so the i-cell beat would be strong. More important, however, for our argument is that, with the same argument as before in Fig. 6*C1*, the e-cells of assembly 2 would, after approximate "delay + spike generation time milliseconds," generate in turn a weak i-beat of assembly 1 that cannot be followed by an e-cell beat. The only possibility for an e-cell beat of assembly 1 to occur is *before* the i-cell beat. However, if we follow this argument for a couple of steps, the period length of the oscillation becomes shorter and shorter, eventually ending at γ rather than at β frequency.

Because a synchronous oscillation *is* consistent with β frequency (Fig. 6), this seems to be the only possibility when long conduction delays are present. We argue that this is true because either *1*) we have the situation of Fig. 6*C2* where some jitter in the system leads to an anti-phase oscillation at γ frequency, or else we have *2*) a situation where the system seems to stay synchronous at β frequency. The main reason for this state of affairs seems to be the above mentioned conditions which lead to i-cell firing *before* possible e-cell activity (on both sites). Given that, even small i-cell activity at a given site will then, due to fast and powerful IPSPs, inhibit e-cell firing at the local site. This should hold for both sites as long as e-cells are inhibited considerably longer than i-cells (so that jitter cannot reverse the firing order of the respective cell groups). Thus long-interval population doublets are generated and the oscillation should stay synchronous. Whether this heuristic stability argument is mathematically correct, and under which conditions (i.e., heterogeneity) this synchronous β oscillation would be stable, could only be proven with a rigorous mathematical analysis, e.g., using maps as in Ermentrout and Kopell (1998) or Kopell et al. (2000). Thus the frequencies and oscillation patterns (i.e., almost anti-phase γ and a synchronous β showing missed e-cell beats) result naturally by considering IPSPs as giving the γ period length and axonal conduction delays as accounting for interactions between the two assemblies. In addition, some conditions regarding ratios of i $\rightarrow$ e and i $\rightarrow$ i conductances and the delay are important.

An (almost) anti-phase oscillation is the most stable oscillation pattern of two assemblies that are separated by axonal conduction delays of approximately one-half a γ period (delays from 8 to 17 ms in our simulations), and that are firing at γ frequency. This is the case, because it is the only configuration in which both a γ oscillation period and also interactions between the two sites are possible. This notion is consistent with the fact that all simulations with average axonal conduction delays of 12 ms (i.e., approximately one-half the γ oscillation period) and firing at γ frequency shown in this paper (Figs. 4*A*, 5*B*, and 7*B*, see also beginning of Fig. 8*B*), display large phase-lags between the two assemblies, yielding almost *anti-phase* oscillations. To show this rigorously and examine necessary and sufficient conditions, again a mathematical analysis would be necessary. We also pointed out that, in these cases, synchrony is impossible, because i $\rightarrow$ e conductances are too small/e-cell IPSPs are too brief to inhibit e-cells longer than "delay + spike generation time milliseconds" (Fig. 4*A*, see also beginning of Fig. 8*B*); or else, i $\rightarrow$ i conductances are too large (Figs. 5*B* and 7*B*), so that an in-phase oscillation at β frequency is impossible. In the case when i $\rightarrow$ e conductances are too small, i-cells produce smaller (population) IPSPs in the e-cells. Because of that, e-cells are not inhibited longer than i-cells, which in turn means that the e-cells fire before the i-cells and activate additional i-cells. In the case when i $\rightarrow$ i conductances are too large, i-cells are inhibited so long that, again, (some) e-cells fire before their respective i-cells, and activate the rest of the i-cells. Thus in both cases, long-interval population doublets—with small i-cell and (almost) no e-cell activity—are not possible, because e-cells fire before i-cells.

A further example of anti-phase activity that confirms the reasoning in Fig. 7*A* is shown in Fig. 7*B*. It displays a simulation with an average delay of 12 ms and with a basket cell $\rightarrow$ e-cell conductance and a basket cell $\rightarrow$ i-cell conductance both of three times the usual values. The average e-cell traces in Fig. 7*Ba* show an almost anti-phase γ oscillation, with the first site leading the second by 8 ms (oscillation period: 22 ms—measured in the auto-correlogram of 300 and 500 ms; interval shown here: 160–230 ms). Why do the two assemblies in this case fire almost in anti-phase and at γ frequency? Here, due to the large basket cell $\rightarrow$ i-cell conductance, i-cells are inhibited about as long as e-cells, whereas in Fig. 6*Bb* the i-cells were more briefly inhibited, and therefore reached their firing threshold to generate the long-interval population doublet. One other reason why the simulation of Fig. 7*B* stabilizes in an almost anti-phase oscillation might be the following. Here, the first i-cell beat seen in Fig. 7*Bb* (thin line) occurs 12 ms after the e-cell beat of the other site (shown as the thin line beat in Fig. 7*Ba*; e-cell and i-cell average peaks were used as measures). This means that this i-cell beat is generated by activation of e-cells from the same site (with a short activation delay) as well as those from the other site (with a long activation delay fitting with the long axonal conduction delay between the two assemblies); thus in Fig. 7*B*, only i-cell singlets occur, but the singlets at either site are generated by synaptic excitation, arriving simultaneously, that is produced by firing at *both* sites. This effect stabilizes a large phase-lag between the two sites, which leads to an almost anti-phase oscillation as seen in Fig. 7*B*. This mechanism, of having i-cell singlets generated by simultaneously impinging EPSPs from firing at the two separate sites, of course only works if the two assemblies fire almost in anti-phase, with a delay approximately matching one-half the oscillation period (8- to 17-ms conduction delays were tested and all led to this kind of oscillation).

This anti-phase oscillation (due to large i $\rightarrow$ i conductances), which is generated by one site's e-cells leading to firing of the other site's i-cells after approximate "delay milliseconds," is independent of e $\rightarrow$ e connections (simulation not shown); this makes sense, as the above mentioned stabilization mechanism works entirely via e $\rightarrow$ i conductances. On the other hand, with i $\rightarrow$ e conductances too small, an anti-phase oscillation is stabilized via e $\rightarrow$ e synapses (data not shown); this also is understandable, as in such a case the e-cells of one site activate the e-cells of the other assembly after approximate "delay +

spike generation time milliseconds," which again stabilizes an anti-phase oscillation.

In the simulation shown in Fig. 4*C*, the two assemblies, separated by an average axonal conduction delay of 17 ms, do not fire in anti-phase but rather are relatively uncorrelated in the beginning. However, after about 600 ms, this oscillation also stabilizes into an anti-phase oscillation, but with multiple peaks in the auto-correlogram (at 23, 29, and 33 ms; data not shown). Thus as argued in Fig. 7, anti-phase is easiest to achieve and most stable, if the average axonal conduction delay is close to one-half the oscillation period, but it is also possible with larger delays. In this latter case, the auto-correlogram usually contains multiple peaks, due to the attempt to generate anti-phase.

In the preceding paragraphs, we argued that in our simulations with long conduction delays an oscillation at β frequencies showing missed e-cell beats cannot be anti-phase. Even so, under these conditions, why do individual e-cells not fire on alternating beats, with alternation patterns randomly distributed between the various cells? Such a situation would probably also be unstable, because then some i-cells would fire before the next e-beat (this would be the second beat of the long-interval population doublet activated by the other site's e-cells which had a strong beat before). If enough i-cells are activated in this way, they might shut off all e-cells and thereby lead to a switch to synchrony. This is a possible explanation for the fact that an oscillation of this sort—i.e., random distribution of e-cell firing phases during synchronized β—was never observed in any of our simulations with long conduction delays.

As for all simulations shown up to this point, in the simulations in Fig. 8, e $\rightarrow$ e connections (if present), and e $\rightarrow$ i connections, are plastic. In addition, i $\rightarrow$ e synapses are also plastic in some simulations, as will be mentioned in the text.

Two assemblies separated by large conduction delays can synchronize their activity without e $\rightarrow$ e connections being present. The presence of e $\rightarrow$ e connections allows, however, for synchronization if other parameters are at inappropriate values for synchronization to occur. Fig. 8*A* shows a simulation similar to the one in Fig. 4*B*: the two assemblies are separated by 12 ms on average, and the basket cell $\rightarrow$ e-cell conductance is fixed at three times the usual value (which made synchronization possible in Fig. 4*B*). In contrast to the simulation in Fig. 4*B*, there are no e $\rightarrow$ e connections present in the simulation shown here in Fig. 8*A*. Note that the two assemblies can still fire synchronously, with an oscillation at β frequency and missed e-cell beats; hence, this kind of synchrony does *not* depend on e $\rightarrow$ e connections. This synchrony is stable during the whole 2-s run.

Figure 8*B* illustrates two assemblies that are initially asynchronous (after 2 synchronous beats at the onset of the simulation), because they are separated by 12 ms on average, and the basket cell $\rightarrow$ e-cell conductance is at the usual value (see Fig. 4*A*). These two assemblies can, however, synchronize their activity, if this basket cell $\rightarrow$ e-cell conductance is potentiated during the course of the simulation. Here, during the first 175 ms, as in all our simulations shown before, all synapses (i.e., also e $\rightarrow$ e and e $\rightarrow$ i synapses) were kept constant to let the system organize itself. Then, plasticity began at all these synapses and the basket cell $\rightarrow$ e-cell synaptic conductances (and e $\rightarrow$ e and e $\rightarrow$ i synapses) began to potentiate (seen in the *bottom panel* of Fig. 8*B*). Basket cell $\rightarrow$ e-cell potentiation used a Hebbian learning rule similar to that used for e $\rightarrow$ e and e $\rightarrow$ i synapses, but with low pre- and postsynaptic Ca^{2+} thresholds (see METHODS). [Recall that with our learning rule, the conductance of an inhibitory synapse is enhanced when IPSPs/Cs are *large* simultaneously with postsynaptic activity, i.e., when both the pre- and the postsynaptic cell are active simultaneously. Although there are hints that synchronous activity of presynaptic i- and postsynaptic e-cells leads to potentiation of i $\rightarrow$ e synapses, because the exact learning rule used at biological i $\rightarrow$ e synapses is unknown, we used a Hebbian rule for basket cell $\rightarrow$ e-cell potentiation to be consistent with the learning rules used for e $\rightarrow$ e and e $\rightarrow$ i synapses. The exact choice of the basket cell $\rightarrow$ e-cell learning rule is not critical because we only use potentiation of the synapses. Also, with the low pre- and postsynaptic Ca^{2+} thresholds used, a similar learning result would be achieved with a purely pre- or postsynaptic rule or a rule increasing the basket cell $\rightarrow$ e-cell dependent on other criteria. That this is true is confirmed by other simulations where AHP conductances were increased in a nonself-organized, non-Hebbian way instead of the basket cell $\rightarrow$ e-cell conductances used here, to synchronize two assemblies separated by large axonal conduction delays (see e.g., Bibbig et al. 2001; Kopell et al. 2000). Also recall that almost anti-phase activity of two cells means that the *somata* of the two cells fire almost in anti-phase. With an axonal conduction delay of x milliseconds between the two cells, an action potential will arrive at the axon terminal of the presynaptic cell after x milliseconds. As our learning rule takes presynaptically induced and postsynaptic $[Ca^{2+}]$ into account, it is not synchrony of *somatic* firing times, but rather near-synchrony of the times when the two signals arrive at the presynaptic and postsynaptic sites that determine whether learning is to take place. The reader should note furthermore, that—as stated above—with our learning rule, simultaneous pre- and postsynaptic activity leads to a *potentiation* of the inhibitory synapse (as observed with tetanic or θ-patterned stimulation; Whittington, unpublished data and Perez et al. 1999), not a depression. Taken together, this means that for long conduction delays, almost anti-phase activity is optimal for learning, because in such a case both the synapse from cell 1 to cell 2, and also a synapse from cell 2 to cell 1, will be potentiated (Bibbig et al. 2001). Such a learning scheme leads to symmetric potentiation of synaptic conductances, which is important for synchrony (Bibbig et al. 2001; Traub et al. 1999).] We chose low thresholds for basket cell $\rightarrow$ e-cell potentiation, because we only wished to see whether the system was able to synchronize its activity after formerly being asynchronous, independent of details of the learning rule. After approximately 350 ms, the two assemblies did indeed synchronize their activity and then stayed synchronous, as in the oscillations shown in previous figures that began and continued synchronously, and again synchrony occurred with an oscillation at β frequency and with missed e-cell beats. This synchrony was stable for the rest of the 2-s run.

Thus enhancing the basket cell $\rightarrow$ e-cell conductance (such that e-cells are inhibited long enough that the delay-dependent long-interval population doublet will be generated before the e-cells fire again; see Figs. 6 and 7) enables the two assemblies to synchronize their activity, even though their activity was

relatively uncorrelated, or on average, (almost) in anti-phase before. Why, and how exactly, two assemblies were not only able to stabilize their synchronous activity (as in Figs. 4–8*A*) but could even synchronize their formerly asynchronous activity, will be shown in Fig. 11.

Figure 8*C* shows a simulation similar to the one shown in Fig. 8*B*. The only difference here is that, as in the simulation of 8*A*, there are no e → e synapses. Despite the absence of all e → e synapses (i.e., within- and between-assembly e → e synapses), the two assemblies can still synchronize their activity: this implies that e → e synapses are not necessary for synchronization to occur after an epoch of relatively uncorrelated or of an almost anti-phase oscillation, *provided that* i → e synaptic conductances grow enough and that delays are long. However, comparison of Fig. 8, *B* and *C*, also shows that ~30% smaller i → e conductances are needed for synchronizing the two assemblies, if e → e synapses are present (and high, as they grow in the simulation shown in Fig. 8*B*). Thus e → e synapses can play a useful role in long-range synchrony, even if they are not absolutely required.

We conclude from the simulations shown in Fig. 8, and numerous similar ones, conducted with the large, detailed neuronal network model or with the small, simple one, that long-range synchronization in this frequency range (35- to 50-ms period, i.e., 20–29 Hz) and with this oscillation pattern (β frequency and missed e-cell beats), is not dependent on the e → e conductance (i.e., the 2 assemblies are able to fire synchronously without any e → e synapses present at all). On the other hand, e → e synapses support/provide synchronization of two assemblies separated by long axonal conduction delays if other parameters are not optimal (i.e., over a range of i → e conductances which themselves are not large enough, or in the presence of an inappropriate tonic drive). Numerous simulations show that this is true for synchrony in simulations when i → e (or basket cell → e-cell) conductances are high from the beginning (e.g., Fig. 8*A*). It is also true in simulations with growing i → e (or basket cell → e-cell) conductances (as shown in Fig. 8*C*) and in simulations with fixed high or growing e-cell AHPs. (Large e-cell AHPs also keep the e-cells inhibited long enough for the i-cells to generate a long-interval population doublet before the e-cells would fire their next beat. There, an oscillation at β frequency (40- to 50-ms period) with skipped e-cell beats is generated (see the synchronous part of Fig. 9 of Bibbig et al. 2001).

Note that in hippocampal slices with relatively short delays, e → e synapses *are* needed for a synchronous, beat-skipping β oscillation to occur. This was shown both experimentally and in compartmental network models (Faulkner et al. 1999; Traub et al. 1999). Furthermore, for synchronization of two assemblies that are separated by large conduction delays, theoretical results and simulations with a small network model (Kopell et al. 2000) indicate that (within a certain parameter regimen) e → e synapses are necessary to prevent anti-phase activity. However, our simulation results with large detailed networks show that e → e synapses are not necessary for synchrony of two assemblies separated by large conduction delays if the i → e conductances (or e-cell AHPs) and e → i conductances are sufficiently high, but e → e conductances can contribute to the generation of synchrony in oscillations that otherwise would be asynchronous due to suboptimal conditions (present results and Bibbig and Traub, unpublished data).

Synchronization of two assemblies after an almost anti-phase oscillation is also possible in networks of simple integrate-and-fire neurons along with plastic e → e, e → i, and i → e synapses. Figure 9 shows a simulation with the simple network model where assembly 1 and assembly 3, which were

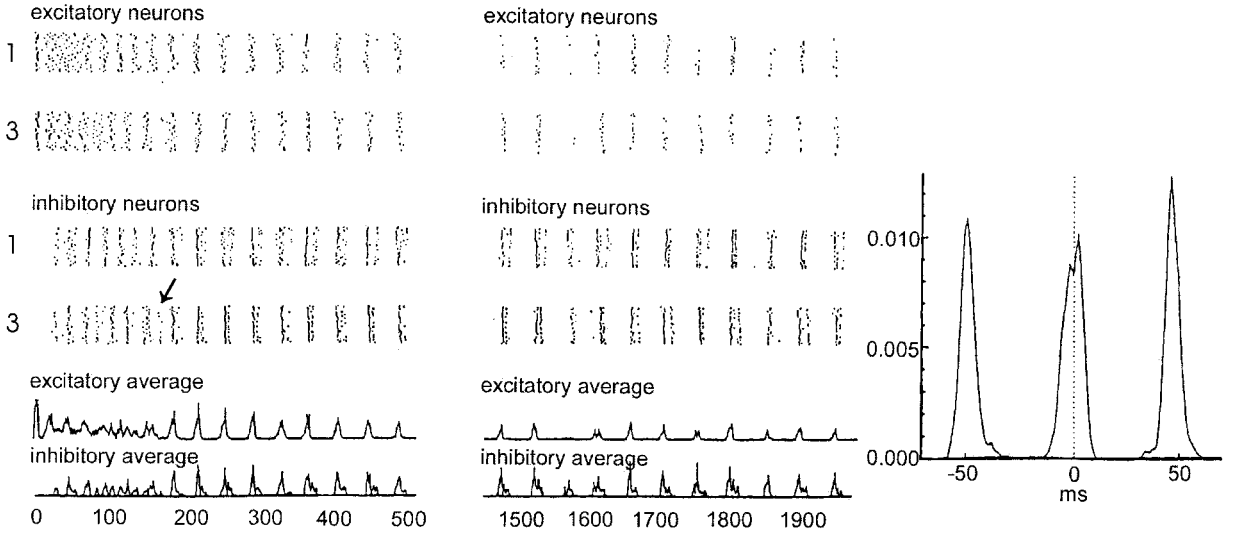

FIG. 9. Synchronization of 2 assemblies firing almost in anti-phase with the help of interneuron plasticity in a network of simple integrate-and-fire neurons. Firing patterns of excitatory neurons (*top*) and inhibitory neurons (*middle*) of two assemblies (assembly 1 and 3) and average activity (*bottom*) of the first (*left*) and the last 500 ms (*middle*) of a 2-s run. The arrow indicates the synchronization-weak-beat (see Fig. 11 for explanation). *Right*: cross-correlogram of the e-cell activity of assembly 1 and 3 during the last 500 ms. In this simulation, assemblies 1 and 3, which are separated by an average "axonal" conduction delay of 8 ms, are excited by a tonic input, and e → e, e → i, and i → e synapses are plastic following a Hebbian learning rule (see METHODS). *Left plot*: after a starting phase of asynchronous activity switching into an almost anti-phase oscillation (cross-correlogram, not shown) assemblies 1 and 3 synchronize their activity after approximately 180 ms. They continued to fire synchronously at β frequency (oscillation period = 48 ms, measured in autocorrelation) for the rest of the 2-s run as indicated by the plot of the firing patterns during (1,500 and 2,000 ms; *middle*) and the cross-correlogram during this time window (*right*).

separated by an average axonal conduction delay of 8 ms, were stimulated simultaneously with a tonic input. Here, e → e, e → i, and i → e synapses were plastic, and after an interval of asynchronous activity in the beginning of the oscillation, the two assemblies synchronized their activity at about 180 ms (left spike plot; in these simulations with simple networks, plasticity started at the beginning of the simulation and not 175 ms after the beginning of the oscillation as in the simulations with networks of detailed neurons). Note that just before synchronization at about 160 ms, assembly 3 generates a beat with a small number of active i-cells, and in this case, no e-cells active (indicated by the arrow, a so-called "i-weak beat"; Bibbig 1999, 2000; Bibbig et al. 2001), which we now call a *synchronizing-weak-beat* to emphasize its function, and because i-cell *and* e-cell activity are sparse in a synchronizing-weak-beat; we will explain in Fig. 11 exactly how a synchronizing-weak-beat can lead to synchronization). The two assemblies remained synchronous until the end of the simulation at 2 s, as seen in the middle spike plot and in the cross-correlogram on the right. In another simulation without e → e-plasticity, and otherwise the same parameters, the two assemblies were able to synchronize after about 190 ms (data not shown). In these simulations, as in all simulations with the simple network, e-cell projections were far-reaching, whereas i-cells only projected locally (i.e., i-cells from assembly 1 could not project to e- and i-cells from assembly 3 and vice versa). That the two assemblies were able to synchronize in these simulations means that local i → e connectivity is sufficient for long-range synchronization (in addition to other prerequisites like between-assembly e → i connections) and even a few between-assembly i → e connections (as used in the simulations with detailed networks shown in this paper; see METHODS) are not necessary.

Synchronization of two assemblies separated by large conduction delays with the help of interneuron plasticity is not simply due to slowing down of the oscillation frequency. Theoretical work suggests that synchronization with axonal conduction delays of more than 6 ms is easier if the carrier frequency is lower (König and Schillen 1991). Therefore one idea as to why the two assemblies in the simulations with interneuron plasticity (Figs. 8, *B* and *C*, and 9) are able to synchronize is this: due to i → e potentiation, the network oscillation simply becomes slower, which then allows synchronization of the two assemblies.

Figure 10, *A* and *B*, shows simulations in which the two assemblies were separated by an average axonal conduction delay of 14 ms but with plasticity at different synapses. As seen here, the situation is more complicated than a simple linear dependence of the synchronization ability on the oscillation period. *If*—for a given delay—only the oscillation frequency would determine whether two assemblies are able to synchronize, then of course, the measure would be the frequency *before* synchronization, because later the synchronization process is already over. Figure 10*A* shows a simulation similar to that shown in Fig. 9 (i.e., e → e, e → i, and i → e synapses were plastic). Here, after about 680 ms, the two assemblies are able to synchronize their activity (*left*). Note again the synchronizing-weak-beat, with smaller i-cell and e-cell activity than usual, just before synchronization (arrow). Before synchronization, the two assemblies fire with an almost anti-phase oscillation. The period length of this oscillation was 28 ms, as

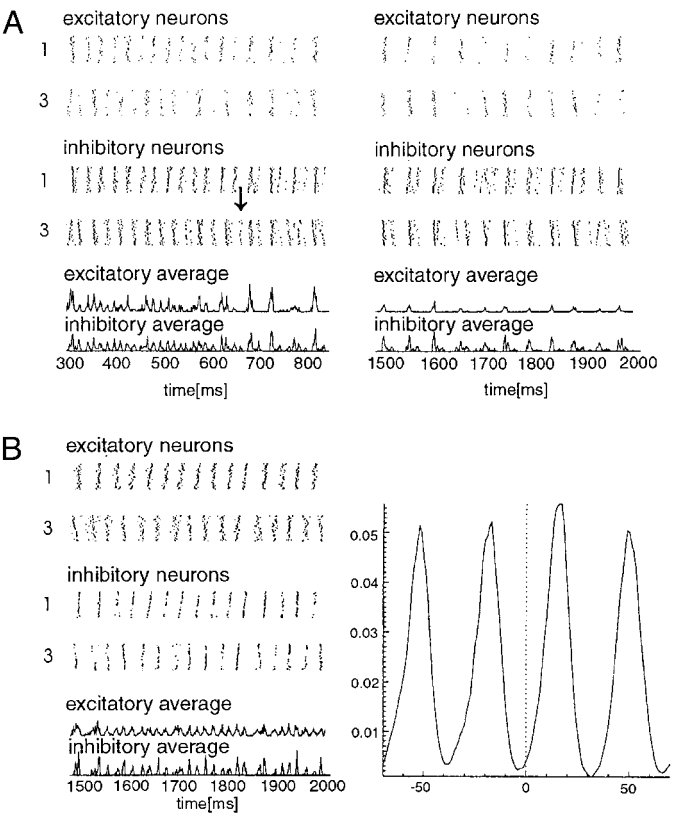

FIG. 10. Synchronization of two assemblies separated by long "axonal" conduction delays with the help of interneuron plasticity is not simply connected with a "linear" dependence of the oscillation frequency on the delay: firing patterns of the assemblies are also important. Simulations with networks of integrate-and-fire neurons similar to the ones shown in Fig. 9. Here assemblies 1 and 3 are separated by an average "axonal" conduction delay of 14 ms. *A*: e → e, e → i, and i → e synapses are plastic. *Left*: spike plots of e-cell activity (*top*) and i-cell activity (*middle*) and average traces (*bottom*) of the interval [300, 850 ms]. *Right*: same for the interval [1,500 and 2,000 ms]. *B*: e → e, i → i, and i → e synapses are plastic (but not e → i). *Left:* spike plots of e-cell activity (*top*) and i-cell activity (*middle*) and average traces (*bottom*) of the interval [1,500 and 2,000 ms]. *Right:* cross-correlogram of e-cell activity of assemblies 1 and 3 during this time. The arrow again indicates the synchronization-weak-beat. *A*: 2 assemblies are able to synchronize their activity after firing in anti-phase for approximately 680 ms. Oscillation period before synchronization: 28 ms. *B*: although the 2 assemblies fire at a lower frequency (period length: 35 ms) than the assemblies shown in *A*, they are not able to synchronize their activity but remain firing at almost anti-phase until the end of the simulation at 2 s, as seen in the spike plot (*left*) and the cross-correlogram of the e-cell groups (*right*). Figure 11 explains why.

seen in the auto-correlogram of the lower group of e-cells (data not shown). In the simulation shown in Fig. 10*B*, where only e → e-, i → e-, and i → i synapses were plastic, but not e → i synapses, the two assemblies stayed in an anti-phase oscillation despite their period being as slow as 35 ms, i.e., a period 7 ms longer than was the case for an oscillation that *was* able to synchronize (Fig. 10*A*). Thus period length is not the sole criterion that determines whether the system can synchronize. We will learn in the next figure why this is the case.

Synchronization with the help of a synchronizing-weak-beat is reached by sudden changes in the oscillation period length of the two assemblies. In Figs. 8*B*, *C*, 9 and 10 we saw that synchronization of two assemblies oscillating almost in anti-phase with each other is possible with the help of interneuron plasticity producing a synchronizing-weak-beat (it is hard to see in this magnification of Fig. 8, but it exists). To see exactly

how this synchronization is generated we first perform a thought experiment by addressing the question "how can we transform an (almost) anti-phase gamma oscillation into a synchronous oscillation?" If we have two assemblies firing almost in anti-phase, then we have two possibilities for synchronizing them: *1*) gradually, i.e., two assemblies firing at different frequencies become more and more synchronized or *2*) a jump from anti-phase to in-phase. All simulations performed with the simple or with the detailed network model showed that the phase-shift between the two assemblies was relatively constant during the beats before synchronization (at least on average, see e.g., Fig. 11), so that possibility *1*) did not occur, and possibility *2*) is left. How does a jump work? If the two assemblies fire almost in anti-phase and then one assembly suddenly generates a cycle of approximately one-half the period of the other, then the two assemblies will become synchronized. As we see in Fig. 11, a *synchronizing-weak-beat* can generate a jump like this.

First, how can i-plasticity lead to a *synchronizing-weak-beat*? With plasticity of i → e and e → i synapses, *1*) e-cells are progressively inhibited longer than i-cells due to i → e potentiation (and i → i synaptic conductances staying at a constant level; local effect), and *2*) due to e → i potentiation, e-cells of one assembly can more and more excite i-cells of the other assembly, after a delay of approximately "conduction delay milliseconds" (2-site effect). Together, *1*) and *2*) allow that in the simulation shown in Fig. 11, some i-cells of assembly 3 are excited by e-cells of assembly 1 *before* e-cells of assembly 3 fire. This holds for the first (not marked) beat of assembly 3, and for beats 3_2 (second marked beat of assembly 3) and 3_4, with no e-cell activity at all in 3_4. i-Cell activity is relatively normal in the first mentioned beats, whereas there are significantly fewer i-cells active in 3_4. This is because the IPSPs generated by these few i-cells, firing before their respective e-cells, prevent more e-cells from being activated, because they inhibit them just before they would be expected to fire their next beat (as in the long-interval population doublet described before, see e.g., Fig. 6); this again prevents more i-cells from being activated via e → i connections (especially in beat 3_4 where there are no active e-cells at all that could possibly activate i-cells) so that here also the i-cell activity is kept small. Thus a *synchronizing-weak-beat* is generated, defined by less spike activity than in previous beats, i.e., <50% of the usual i-cell action potentials, and only a few or no active e-cells. [Often the activity of one of the two groups, e- or i-cells, is smaller than usual during a few beats before the synchronizing-weak-beat, mostly, as in the simulation shown in Fig. 11, the e-cell activity. A *synchronizing-weak-beat* is characterized by a smaller activity of *both* cell groups.]

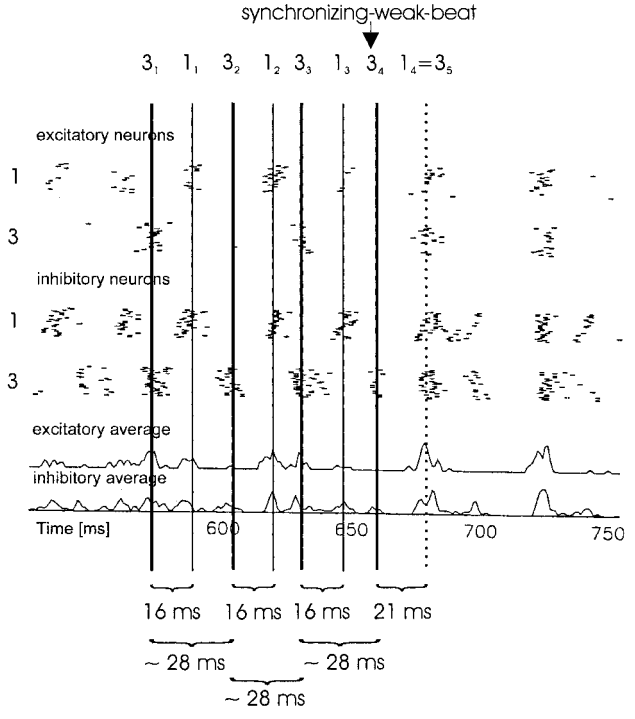

FIG. 11. Synchronization of two widely separated assemblies is generated by a sudden change in the oscillation period length induced by a synchronizing-weak-beat. Excerpt of the spike plots already seen in Fig. 10*A* with a higher time resolution (simple network, 14-ms average delay between the assemblies, e → e, e → i, and i → e synapses are plastic). Single beats are "marked" for example as 3_1, relating to the first marked beat of assembly 3. Beat 3_4 is a synchronizing-weak-beat characterized by fewer i-cell spikes and (here) no e-spikes at all. Note, that *before* the synchronizing-weak-beat, assembly 3 generates an oscillation with an almost constant period length of 28 ms, and assembly 3 leads assembly 1 by 16 ms. *Directly after* the synchronizing-weak-beat, the period length of assembly 3 is reduced to 21 ms, which is also the lead of assembly 3 relative to assembly 1. The period length of assembly 1 is enhanced to 33 ms, so that the 2 assemblies synchronize their activity. See text for explanation of the synchronizing mechanism.

As only 50% or fewer of the usual i-cell spikes are generated during a *synchronizing-weak-beat*, the population IPSP is smaller/shorter, so that e-cells of the ipsilateral assembly 3 are inhibited for a briefer interval than usual. This means that assembly 3 generates a period of shorter duration than usual, 21 ms instead of 28 ms in the periods before. In addition, as fewer e-cells than usual are active during a *synchronizing-weak-beat*, these cells are not able to activate the cells of the contralateral assembly to advance their firing. Consequently, in Fig. 11, after the *synchronizing-weak-beat* of assembly 3, e-cells of assembly 1 are not excited by e-cells of assembly 3 (which had happened in all previous γ periods and thereby led to shortening of these periods). Assembly 1 thus generates a period of longer duration than usual (33 ms instead of 28 ms), which leads to coarse synchronization of the two assemblies. Synchronization is then stabilized later on by broad i-doublets, slowing the oscillation down to β frequency, and generating long-interval population doublets (shown to be necessary for long-range synchronization, e.g., in Fig. 6).

In summary, in the simulation with the simple network shown in Fig. 11, synchronization after an almost anti-phase oscillation is achieved by a *synchronizing-weak-beat* producing a longer oscillation period of one assembly and a shorter one of the other. Synchronization in networks of detailed compartmental neurons is generated according to a similar principle, i.e., with a *synchronizing-weak-beat* (introduced in Bibbig et al. 2001) and a sudden relative change in period length of one assembly compared with the other (e.g., Fig. 8, *B* and *C*).

After learning in Fig. 11 how exactly a synchronizing-weak-beat works, we now are also able to explain why the two assemblies in Fig. 10*B* were unable to synchronize their activity: they were unable to synchronize because the e → i-conductance was not large enough for e-cells of one assembly to excite i-cells of the other assembly. Also, due to i → i potentiation, i-cells were inhibited as long as e-cells were. So

i-cells of either assembly could never be excited *before* the e-cells of the same ipsilateral assembly. Therefore a *synchronizing-weak-beat* with a small number of active i-cells *and* almost no active e-cells was not possible (cf. Fig. 11).

In summary, Figs. 9–11 show that, in very simple network models, potentiation of e → i, and i → e conductances allows for long-range synchronization after an epoch of almost anti-phase oscillation (Figs. 9, 10*A*, and 11). And, as mentioned before, large enough fixed i → e conductances generate synchrony of the two oscillating assemblies from the very beginning of the oscillation (data not shown). Because this synchrony/synchronization only seems to require that *1*) e-cells are inhibited long enough for the (delay-dependent) long-interval population doublet/synchronizing-weak-beat to occur before the next beat of the e-cells, and *2*) it is possible with different network models and different means to achieve the above mentioned prerequisite (i.e., large i → e conductances or AHPs), such a mechanism might also work in the in vitro or in vivo neocortex and under different temporal and spatial conditions. We emphasize that synchronization is possible with relatively simple integrate-and-fire neurons with refractory period or large models with detailed compartmental neurons. Networks with some i → e and i → i connections between the assemblies can be synchronized, as can those with purely local i → e and i → i conductances. So can networks with or without e → e synapses—perhaps representing areas with more or with fewer recurrent pyramidal cell connections.

DISCUSSION

The paper contains five main results about long-range synchronization, i.e., the ability of two assemblies to synchronize their oscillatory activity despite being separated by long axonal conduction delays (~8 ms and above, the exact value depending on parameter choices).

1. Under the conditions studied in this paper (i.e., networks with e- and i-cells both receiving tonic input, long axonal conduction delays, and relatively realistic connectivity), the ability of two assemblies to oscillate synchronously mainly depends on their capability to generate *long-interval population doublets*, a concept introduced in this paper. A long-interval doublet is defined as a pair of interneuron action potentials—separated by approximately "delay + spike generation time milliseconds"—in which *1*) the first action potential is induced by tonic inputs and/or excitation from nearby e-cells, while *2*) the second action potential is induced by (delayed) excitation from distant e-cells. A long-interval population doublet is defined as a long-interval doublet of (almost) all i-cells. Such a long-interval population doublet then inhibits the local e-cells, which leads to a firing pattern of i-cells firing every γ period while e-cells fire on every second γ period (and hence skip alternate beats and fire at β frequency; see Figs. 3*Bc* and 6*C*).
2. Two assemblies (separated by large axonal conduction delays) firing with an oscillation pattern of skipped e-cell beats will fire (almost) synchronously, i.e., in-phase, at β frequency (see Figs. 3*Bc* and 6), whereas they fire with a large phase lag or (almost) in anti-phase at γ frequency if long-interval population doublets, and thus the skipped e-cell beats, are absent (see Figs. 3*Bb* and 7).
3. For long-interval doublets/long-interval population doublets to be present, i → e conductance (in relation to i → i conductance) and/or e-cell AHPs have to be large enough (local, 1-site effect). The necessary values depend on the axonal conduction delay between the two assemblies, i.e., the higher the delay the larger the i → e conductance and/or e-cell AHP necessary for long-interval population doublets and thus synchrony to be possible. As in neocortex and hippocampus, the i → e conductance really is larger than the i → i conductance (e.g., Tamás et al. 2000), and because there is only potentiation of i → e and, with one exception, not i → i conductances, long-interval population doublets should be possible. Another prerequisite for long-interval population doublets in addition to large/long enough i → e conductances is that e → i conductances be large enough for e-cells of one assembly to excite i-cells of the other assembly (2-site effect). At least in the hippocampus, this condition might be fulfilled as e → i conductances are large (Gulyás et al. 1993; Miles 1990) and there are at least a few long-range e → i conductances (Melchitzky et al. 1998, 2001).
4. Two assemblies firing with large phase lags or (almost) in anti-phase due to conditions not sufficient to generate long-interval population doublets (see 2 and 3 above), can synchronize their oscillatory activity with the help of interneuron plasticity (here potentiation of e → i and i → e conductances), which can switch the activity from anti-phase to in-phase. Interneuron plasticity here guarantees that *1*) the e → i conductance will be large enough for e-cells of one assembly to excite i-cells of the other one and that *2*) the i → e conductance is larger than the i → i conductance so that e-cells will be inhibited longer than i-cells. *1*) and *2*) consequently enable the assemblies to generate a synchronizing-weak-beat, which leads to coarse synchrony. Finally, stable fine synchronization is accomplished by long-interval population doublets.
5. The delay-dependent mechanism introduced here for long-range synchronization at β frequency thus mainly depends on the pyramidal-interneuron-pyramidal network (e-i-e network), with large enough long-range (i.e., between-assembly) pyramidal-interneuron connections being important for activation of the other assembly, and delay-dependent large enough local i → e conductances (or AHPs) (compared with i → i conductances) being responsible for suppressing pyramidal cells longer than interneurons. When the array is split in two, so that long-range e → i connections no longer exist, nor any other long-range interactions, then the two sides oscillate independently at γ frequency, not β (data not shown). Thus the β we describe here is generated by two-site interactions.

Our results agree with hippocampal in vitro experiments, and with clinical and theoretical results, indicating that two areas separated by long axonal conduction delays can synchronize at β but not at γ frequency (e.g., Kopell et al. 2000, Tallon-Baudry et al. 1998, 1999, 2001, von Stein et al. 1999). In Tallon-Baudry et al. (2001), for example, two locally restricted assemblies in widely separated areas (several centimeters), involved in a short-term memory task, oscillate at different γ frequencies before synchronizing at β frequency. As this

characteristic fits well with our data, the two sides might synchronize using the synchronization mechanism proposed here, if the (yet unknown) axonal conduction velocities of these connections are not too large and not too small. But there is also a small difference in the results of Tallon-Baudry et al. (2001) with our simulations regarding the asynchronous phase: in our simulations, the two assemblies fire at the same γ frequency but with an almost one-half period phase lag and then synchronize at β frequency. A slightly larger difference in the tonic drive of the two assemblies might also generate different firing frequencies, and activity of more than two simultaneously firing assemblies might additionally help to generate different phase-shifts or even frequencies between the assemblies. It should be noted that there are, however, data demonstrating synchronous γ frequency oscillations involving areas separated by large distances, up to several centimeters. (e.g., Desmedt and Tomberg 1994). Such synchronization might be possible if the respective areas are interconnected by fast-conducting fibers that run in the white matter. In such a case, the interconnection delays would be only a few milliseconds. Our results apply best to situations in which the interconnecting fibers run within the gray matter and conduct at relatively slow velocity, so as to produce long between-assembly delays.

Furthermore, theoretical results and simulations with compartmental neurons suggest that synchronization with mean axonal conduction delays of more than 5 or 6 ms is unreliable if possible at all (Bush and Sejnowski 1996; Ritz et al. 1994) but is easier if the carrier frequency is lower (e.g., König and Schillen 1991). In accordance with this, we showed that for a synchronous oscillation to occur in our networks, the necessary i $\rightarrow$ e conductance (and, consequently, the oscillation period) increases with the delay (e.g., Fig. 4). Comparison of synchronization times in Figs. 9 and 10*A* with average conduction delays of 8 and 14 ms, respectively, also show this dependence (the low-threshold learning rule used for i $\rightarrow$ e synapses is at least roughly translatable to potentiation of i $\rightarrow$ e conductances). We also argued why this is the case, namely because stable synchrony with large axonal conduction delays requires *long-interval population doublets*, which again require larger i $\rightarrow$ e conductances for larger delays. For synchronization after an (almost) anti-phase oscillation a *synchronizing-weak-beat* is necessary. Taken together, this means that a small enough firing frequency/large enough oscillation period is necessary but not sufficient for stable synchrony or—if the two assemblies initially fire almost in anti-phase—synchronization. This means in particular that if there is no long-interval population doublet or synchronizing-weak-beat, respectively, then the two assemblies fire in almost anti-phase despite a low oscillation frequency: Thus it is possible that, with the same delay of 14 ms on average between the two assemblies, two assemblies oscillate with a period length of 35 ms and fire in anti-phase (if long-interval population doublets and/or synchronizing-weak-beats are impossible), or else they can synchronize their activity to in-phase originally firing with a smaller period length, e.g., 28 ms (e.g., Fig. 10, *B* and *A*, respectively).

How exactly do the different synaptic conductances influence long-range synchrony? A high enough e $\rightarrow$ i conductance is one necessary condition, allowing for synchronization of two asynchronously firing assemblies (via activating some i-cells of the other assembly, producing one necessary condition for a synchronizing-weak-beat), and once established, stabilizing synchrony (again via activating the other assembly's i-cells, thus making long-interval population doublets possible). The same holds for i $\rightarrow$ e synapses: a high enough i $\rightarrow$ e conductance/long enough e-cell IPSP is necessary to stabilize synchronization (via inhibiting e-cells longer than i-cells, allowing for long-interval population doublets) once the two assemblies fire synchronously. [The high i $\rightarrow$ e conductance could be replaced by a large enough e-cell AHP.] In addition, a high enough i $\rightarrow$ e conductance/long enough e-cell IPSP is necessary for synchronizing two asynchronously firing assemblies (via inhibiting local e-cells, thus also making a synchronizing-weak-beat possible). On the other hand, excessively high e $\rightarrow$ e and i $\rightarrow$ i conductances (and low e $\rightarrow$ i or i $\rightarrow$ e conductances) seem to stabilize almost half-period phase lags or anti-phase oscillations, in oscillations with long axonal conduction delays between the two assemblies, by preventing the above mentioned necessary conditions.

Intermediate e $\rightarrow$ e conductances might help long-distance synchronization, e.g., in cases where i $\rightarrow$ e synapses are not large enough (see Fig. 8). Such e $\rightarrow$ e conductances, however, are not necessary for long-distance synchronization under otherwise optimal conditions in which long-interval population doublets or synchronizing-weak-beats are possible [i.e., i $\rightarrow$ e synaptic conductances large enough compared with i $\rightarrow$ i conductances and to the delay, so as to inhibit e-cells longer than i-cells (Fig. 8), or e-cell AHPs larger than i-cell AHPs to produce the same result; Bibbig, unpublished data].

The relation between the different conductances is drive-dependent, because in our simulations, i-cells receive less tonic input than e-cells (simulating the smaller metabotropic, tonic activation of i-cells compared with e-cells in hippocampal slices induced by tetanic stimulation; Whittington et al. 1997a). So it might actually be that a lower tonic input to principal cells can allow for synchronization, whereas a higher one generates an asynchronous oscillation. This is the reason why we sometimes observe synchronization some time after synaptic weights reached their maximum during plasticity. In our simulations, after 800 ms, the drive to e-cells and i-cells goes down linearly to 55% of their maximum values. This might change the ratio of e-cell and i-cell drive, favoring i-cells, and thus enabling i-cells to fire before e-cells and a synchronizing-weak-beat (Bibbig, unpublished results). As changes in a synchronous oscillation in the brain are thought to be quite fast, i.e., occur within a few beats, i-plasticity seems to be more likely to produce synchronization than are relatively slow changes of the metabotropic drive.

Why do we use i $\rightarrow$ e plasticity (in addition to e $\rightarrow$ e and e $\rightarrow$ i plasticity) in some of our simulations? First, e-cell IPSPs appear to increase during the course of a γ oscillation (Whittington, unpublished data) and i $\rightarrow$ e plasticity in the hippocampus was also shown before by others (e.g., posttetanic potentiation by Jensen et al. 1999; long-term potentiation by Perez et al. 1999). Second, the measured e-cell IPSPs in a silent, i.e., not oscillating, slice (known from paired recordings) are quite a bit smaller than the ones needed here for long-range synchronization. Thus a gradual potentiation to a higher i $\rightarrow$ e conductance, i.e., plasticity, seems much more likely than a jump. Furthermore, large e-cell IPSPs in the beginning make a γ oscillation unstable (e.g., Bibbig 2000), whereas they are necessary for synchronization over long dis-

tances (see Bibbig 1998, 2000 and this paper for simulations with simple integrate-and-fire neurons, and this paper for simulations with networks of detailed compartmental cells), so a mechanism for i → e potentiation (at the same time as when e → e and e → i synaptic conductances also grow) seems possible and necessary. These reasons are all still valid, when e-cell AHPs play a role—in addition to large i → e conductances—in synchronizing two assemblies separated by long axonal conduction delays, as in that case the required i → e conductances are smaller; even so, a potentiation from resting values is needed to obtain long-range synchrony. We usually use these resting values for unitary conductances in our simulations because they are the only ones experimentally known from paired recordings. We know that population IPSPs (and EPSPs) and thus unitary conductances grow during an experimental oscillation, but we cannot quantitate how much the unitary conductances grow.

This paper offers a purely cortical mechanism for synchronization of two areas separated by large conduction delays (≥8 ms) and oscillating at β frequency, unlike for example, long-range synchronization of spindles that is thought to be performed via thalamo-cortical and cortico-thalamic interactions (Destexhe et al. 1998). Furthermore, contrary to large-scale synchronization of spindles, synchronization of oscillations at 30–40 Hz in the thalamo-cortical system seem to be spatially confined (Steriade et al. 1996), at least under anesthesia, whereas we try to explain with our models real long-range synchronization of neocortical oscillations at 20–30 Hz (often closer to 30 Hz).

One (at least in principle) experimentally testable prediction of our simulations is that if two assemblies fire at γ frequency with an almost one-half period phase lag, they should synchronize suddenly and then switch to β frequency and stay synchronized. Closer inspection of the firing patterns of e- and i-cells should reveal a synchronizing-weak-beat and long-interval population doublets.

We thank G. Palm, A. Knoblauch, T. Wennekers, N. Kopell, K. Rockland, B. Wong, R. Bianchi, E. Buhl, and C. Gray for valuable discussions, T. Wennekers for developing a neural network simulator, B. Walkup for help with the parallel computer, and G. Palm for invaluable support over many years. Also, we thank our anonymous referees for helpful comments.

This work was supported by the Wellcome Trust, the Deutsche Forschungsgemeinschaft, and the Medical Research Council (MRC), U.K. Some of the simulations were performed at the University of Birmingham (U.K.) and at the University of Ulm (Germany). R. D. Traub was a Wellcome Principal Research Fellow, and A. Bibbig is a Wellcome Postdoctoral Fellow.

REFERENCES

ARONIADOU VA AND KELLER A. The patterns and synaptic properties of horizontal intracortical connections in the rat motor cortex. *J Neurophysiol* 70: 1553–1569, 1993.

ARTOLA A, BRÖCHER S, AND SINGER W. Different voltage-dependent thresholds for inducing long-term depression and long-term potentiation in slices of rat visual cortex. *Nature* 347: 69–72, 1990.

BIBBIG A. Cell assemblies and the plasticity of inhibitory and excitatory cells and synapses—a computer model. *Soc Neurosci Abstr* 24: 329,1998.

BIBBIG A. $\gamma \rightarrow \beta$ transition, pattern separation and the plasticity of inhibitory and excitatory synapses. *Soc Neurosci Abstr* 25: 2257, 1999.

BIBBIG A. Oszillationen Synchronisation Mustertrennung und Hebb'sches Lernen inNetzwerken aus erregenden und hemmenden Neuronen. (PhD dissertation). Germany: University of Ulm, 2000.

BIBBIG A, FAULKNER HJ, WHITTINGTON MA, AND TRAUB RD. Self-organized synaptic plasticity contributes to the shaping of γ and β oscillations in vitro. *J Neurosci* 21: 9053–9067, 2001.

BIBBIG A AND TRAUB RD. Interneuron weak beats provide coarse synchrony, and doublets stabilize fine synchrony, of gamma oscillations in networks with long axon conduction delays. *Soc Neurosci Abstr* 26: 1965, 2000.

BIENENSTOCK EL, COOPER LN, AND MUNRO PW. Theory for the development of neuron selectivity: orientation specificity and binocular interaction in visual cortex. *J Neurosci* 2: 32–48, 1982.

BUSH P AND SEJNOWSKI T. Inhibition synchronizes sparsely connected cortical neurons within and between columns in realistic network models. *J Comput Neurosci* 3: 91–110, 1996.

CHAPMAN CA, WOODHALL GL, AND LACAILLE J-C. Long-lasting potentiation of monosynaptic $GABA_A$ IPSPs by theta stimulation in CA1 hippocampal pyramidal cells. *Soc Neurosci Abstr* 25: 735, 1999.

CSICSVÁRI J, HIRASE H, CZURKO A, AND BUZSÁKI G. Reliability and state dependence of pyramidal cell-interneuron synapses in the hippocampus: an ensemble approach in the behaving rat. *Neuron* 21: 179–189, 1998.

DESMEDT JE AND TOMBERG C. Transient phase-locking of 40 Hz electrical oscillations in prefrontal and parietal human cortex reflects the process of conscious somatic perception. *Neurosci Lett* 168: 126–129, 1994.

DESTEXHE A, CONTRERAS D, AND STERIADE M. Mechanisms underlying the synchronizing action of corticothalamic feedback through inhibition of thalamic relay cells. *J Neurophysiol* 79, 999–1016, 1998.

DRAGOI G, HIRASE H, AND BUZSÁKI G. Changes in spontaneous discharge rates of hippocampal neurons by LTP and LTD. *Soc Neurosci Abstr* 26: 183, 2000.

ECKHORN R, BAUER R, JORDAN W, BROSCH M, KRUSE W, MUNK M, AND REITBOECK HJ. Coherent oscillations: a mechanism of feature linking in the visual cortex? *Biol Cybern* 60: 121–130, 1988.

ECKHORN R, FRIEN A, BAUER R, WOELBERN T, AND KEHR H. High frequency (60–90 Hz) oscillations in primary visual cortex of awake monkey. *Neuroreport* 4: 243–246, 1993.

ERMENTROUT GB AND KOPELL N. Fine structure of neural spiking and synchronization in the presence of conduction delays. *Proc Natl Acad Sci USA* 95: 1259–1264, 1998.

FAULKNER HJ, TRAUB RD, WHITTINGTON MA. Anaesthetic/amnesic agents disrupt beta frequency oscillations associated with potentiation of excitatory synaptic potentials in the rat hippocampal slice. *Br J Pharmacol* 128: 1813–1825, 1999.

FRIEN A, ECKHORN R, BAUER R, WOELBORN T, AND KEHR H. Stimulus-specific fast oscillations at zero phase between visual areas V1 and V2 of awake monkey. *Neuroreport* 5: 2273–2277, 1994.

GEIGER P JR., ROTH A, TASKIN B, AND JONAS P. Glutamate-mediated synaptic excitation of cortical interneurons. In: *Handbook of Experimental Pharmacology, Vol. 141: Ionotropic Glutamate Receptors in the CNS*, edited by Jonas P and Monyer H, New York: Springer Verlag, 1999, p. 363–398.

GRAY CM. Synchronous oscillations in neuronal systems: mechanisms and functions. *J Comput Neurosci* 1: 11–38, 1994.

GRAY CM, KÖNIG P, ENGEL AK, AND SINGER W. Oscillatory responses in cat visual cortex exhibit inter-columnar synchronization which reflects global stimulus properties. *Nature* 338: 334–337, 1989.

GRAY CM AND SINGER W. Stimulus-specific neuronal oscillations in orientation columns of cat visual cortex. *Proc Natl Acad Sci USA* 86: 1698–1702, 1989.

GRUNZE CR, RAINNIE DG, HASSELMO ME, BARKAI E, HEARN EF, MCCARLEY RW, AND GREENE RW. NMDA-dependent modulation of CA1 local circuit inhibition. *J Neurosci* 16: 2034–2043, 1996.

GULYÁS AI, MILES R, SIK A, TÓTH K, TAMAMAKI N, AND FREUND TF. Hippocampal pyramidal cells excite inhibitory neurons through a single release site. *Nature* 366: 683–687, 1993.

HOLMGREN CD AND ZILBERTER Y. Coincident spiking activity induces long-term changes in inhibition of neocortical pyramidal cells. *J Neurosci* 21: 8270–8277, 2001.

JENSEN K, JENSEN MS, AND LAMBERT JDC. Post-tetanic potentiation of GABAergic IPSCs in cultured rat hippocampal neurones. *J Physiol (Lond)* 519: 71–84, 1999.

KOESTER HJ AND SAKMANN B. Calcium dynamics in single spines during coincident pre- and postsynaptic activity depend on relative timing of back-propagating action potentials and subthreshold excitatory postsynaptic potentials. *Proc Natl Acad Sci USA* 95: 9596–9601, 1998.

KÖNIG P AND SCHILLEN TB. Stimulus-dependent assembly formation of oscillatory responses: I. Synchronization. *Neural Comput* 3: 155–166, 1991.

KOPELL N, ERMENTROUT GB, WHITTINGTON MA, AND TRAUB RD. Gamma rhythms and beta rhythms have different synchronization properties. *Proc Natl Acad Sci USA* 97: 1867–1872, 2000.

KREITER AK AND SINGER W. Stimulus-dependent synchronization of neuronal responses in the visual cortex of the awake macaque monkey. *J Neurosci* 16: 2381–2396, 1996.

MELCHITZKY DS, GONZALEZ-BURGOS G, BARRIONUEVO G, AND LEWIS DA. Synaptic targets of the intrinsic axon collaterals of supragranular pyramidal neurons in monkey prefrontal cortex. *J Comp Neurol* 430: 209–221, 2001.

MELCHITZKY DS, SESACK SR, PUCAK ML, AND LEWIS DA. Synaptic targets of pyramidal neurons providing intrinsic horizontal connections in monkey prefrontal cortex. *J Comp Neurol* 390: 211–224, 1998.

MILES R. Synaptic excitation of inhibitory cells by single CA3 hippocampal pyramidal cells of the guinea-pig *in vitro*. *J Physiol (Lond)* 428: 61–77, 1990.

MILTNER WHR, BRAUN C, ARNOLD M, WITTE H, AND TAUB E. Coherence of gamma-band EEG activity as a basis for associative learning. *Nature* 397: 434–436, 1999.

MIYAKAWA H, LEV-RAM V, LASSER-ROSS N, AND ROSS WN. Calcium transients evoked by climbing fibre and parallel fibre synaptic inputs in guinea pig cerebellar Purkinje neurons. *J Neurophysiol* 68: 1178–1189, 1992.

NAKAMURA T, BARBARA J-G, NAKAMURA K, AND ROSS WN. Synergistic release of Ca^{2+} from IP_3-sensitive stores evoked by synaptic activation of mGluRs paired with backpropagating action potentials. *Neuron* 24: 727–737, 1999.

NAKAMURA T, NAKAMURA K, LASSER-ROSS N, BARBARA J-G, SANDLER VM, AND ROSS WN. Inositol 1,4,5-triphosphate (IP_3)-mediated Ca^{2+} release evoked by metabotropic agonists and backpropagating action potentials in hippocampal CA1 pyramidal neurons. *J Neurosci* 20: 8365–8376, 2000.

OUARDOUZ M AND LACAILLE J-C. Mechanisms of selective long-term potentiation of excitatory synapses in stratum oriens/alveus interneurons of rat hippocampal slices. *J Neurophysiol* 73: 810–819, 1995.

PEREZ Y, CHAPMAN CA, WOODHALL G, ROBITAILLE R, AND LACAILLE JC. Differential induction of long-lasting potentiation of inhibitory postsynaptic potentials by theta patterned stimulation versus 100-Hz tetanization in hippocampal pyramidal cells in vitro. *Neuroscience* 90: 747–757, 1999.

PEREZ Y, MORIN F, AND LACAILLE JC. A hebbian form of long-term potentiation dependent on mGluR1a in hippocampal inhibitory interneurons. *Proc Natl Acad Sci USA* 98: 9401–9406, 2001.

POZZO-MILLER LD, CONNOR JA, AND ANDREWS SB. Microheterogeneity of calcium signalling in dendrites. *J Physiol (Lond)* 525: 53–61, 2000.

RITZ R, GERSTNER W, FUENTES U, AND VAN HEMMEN JL. A biologically motivated and analytically soluble model of collective oscillations in the cortex. II. Application to binding and pattern segmentation. *Biol Cybern* 71: 349–358, 1994.

ROCKLAND KS AND DRASH GW. Collateralized divergent feedback connections that target multiple cortical areas. *J Comp Neurol.* 373: 529–548, 1996.

ROZOV A, ZILBERTER Y, WOLLMUTH LP, AND BURNASHEV N. Facilitation of currents through rat Ca^{2+}-permeable AMPA receptor channels by activity-dependent relief from polyamine block. *J Physiol (Lond)* 511: 361–377, 1998.

SABATINI BL, OERTNER TG, AND SVOBODA K. The life cycle of Ca^{2+} ions in dendritic spines. *Neuron* 33: 439–452, 2002

SINGER W AND GRAY CM. Visual feature integration and the temporal correlation hypothesis. *Annu Rev Neurosci* 18: 555–586, 1995.

SJÖSTRÖM J, TURRIGIANO GG, AND NELSON SB. Rate, timing, and cooperativity jointly determine cortical synaptic plasticity. *Neuron* 32: 1149–1164, 2001.

STANTON PK AND SEJNOWSKI TJ. Associative long-term depression in the hippocampus induced by hebbian covariance. *Nature* 339: 215–218, 1989.

STERIADE M, CONTRERAS D, AMZICA F, AND TIMOFEEV I. Synchronization of fast (30-40 Hz) spontaneous oscillations in intrathalamic and thalamocortical networks. *J Neurosci* 16, 2788–2808, 1996.

SWADLOW HA. Information flow along neocortical neurons. In: *Time and the Brain*, edited by Miller R. Amsterdam: Harwood Academic Publishers, 2000, p 131–155.

TALLON-BAUDRY C, BERTRAND O, AND FISCHER C. Oscillatory synchrony between human extrastriate areas during visual short-term memory maintenance. *J Neurosci* 21: 1–5, 2001.

TALLON-BAUDRY C, BERTRAND O, PERONNET F, AND PERNIER J. Induced gamma-band activity during the delay of a visual short-term memory task in humans. *J Neurosci* 18: 4244–4254, 1998.

TALLON-BAUDRY C, KREITER A, AND BERTRAND O. Sustained and transient oscillatory responses in the gamma and beta bands in a visual short-term memory task in humans. *Vis Neurosci* 16: 449–459, 1999.

TAMÁS G, BUHL EH, LORINCZ A, AND SOMOGYI P. Proximally targeted GABAergic synapses and gap junctions synchronize cortical interneurons. *Nature Neurosci* 3: 366–371, 2000.

TRAUB RD, JEFFERYS JGR, MILES R, WHITTINGTON MA, AND TÓTH K. A branching dendritic model of a rodent CA3 pyramidal neurone. *J Physiol (Lond)* 481: 79–95, 1994.

TRAUB RD AND MILES R. Pyramidal cell-to-inhibitory cell spike transduction explicable by active dendritic conductances in inhibitory cell. *J Comput Neurosci* 2: 291–298, 1995.

TRAUB RD, WHITTINGTON MA, BUHL EH, JEFFERYS JGR, AND FAULKNER HJ. On the mechanism of the $\gamma \rightarrow \beta$ frequency shift in neuronal oscillations induced in rat hippocampal slices by tetanic stimulation. *J Neurosci* 19: 1088–1105, 1999.

TRAUB RD, WHITTINGTON MA, STANFORD IM, AND JEFFERYS JGR. A mechanism for generation of long-range synchronous fast oscillations in the cortex. *Nature* 383: 621–624, 1996.

VON STEIN A, RAPPELSBERGER P, SARNTHEIN J, AND PETSCHE H. Synchronization between temporal and parietal cortex during multimodal object processing man. *Cereb Cortex* 9: 137–150, 1999.

WHITTINGTON MA, STANFORD IM, COLLING SB, JEFFERYS JGR, AND TRAUB RD. Spatiotemporal patterns of γ frequency oscillations tetanically induced in the rat hippocampal slice. *J Physiol (Lond)* 502: 591–607, 1997a.

WHITTINGTON MA, TRAUB RD, FAULKNER HJ, STANFORD IM, AND JEFFERYS JGR. Recurrent excitatory postsynaptic potentials induced by synchronized fast cortical oscillations. *Proc Natl Acad Sci USA* 94: 12198–12203, 1997b.

YUSTE R AND DENK W. Dendritic spines as basic functional units of neuronal integration. *Nature* 375: 682–684, 1995.